THE DEVELOPMENT OF BETA-ACTIN MUTANTS WITH ALTERED BINDING AFFINITES FOR ATP AND ADP

By

Abu-Bakarr Kuyateh

November, 2018

Director of Thesis: Robert Hughes

Major Department: Chemistry

A number of neurodegenerative diseases are accompanied by the formation of cofilin-actin rods in neural cells. These rods can cause synaptic dysfunction and block transport within neurites. The overall goal of this project is to create an optogenetic switch that incorporates both cofilin (an actin-binding protein) and actin for the study of cofilin-actin rod formation in neural cells undergoing oxidative stress. During the course of the work, a protocol has been created to express the protein β-actin. Protein overexpression and purification, circular dichroism, mass spectrometry, and electrophoresis have been utilized to isolate and characterize β-actin. Site-directed mutagenesis has been conducted to create a series of mutants to explore which residues are key for nucleotide binding. A number of challenges related to protein expression and stability of this protein precluded completion of these studies. As a result, we turned to mutants of optogenetic actin to study nucleotide binding in cells. The results from these studies indicate that point mutants in our actin construct, in conjunction with an optogenetic cofilin, can provide insight into the nucleotide binding state of actin under different oxidant concentrations.

The Development of Beta-Actin Mutants with Altered Binding Affinities for ATP and ADP.

A Thesis

Presented To the Faculty of the Department of Chemistry

East Carolina University

In Partial Fulfillment of the Requirements for the Degree

Master of Science in Chemistry

by

Abu-Bakarr Kuyateh

November , 2018

THE DEVELOPMENT OF BETA-ACTIN MUTANTS WITH ALTERED BINDING AFFINITES FOR ATP AND ADP

by

Abu-Bakarr Kuyateh

APPROVED BY:

DIRECTOR OF
THESIS: _____
Dr. Robert Hughes, Ph.D.

COMMITTEE MEMBER: _____
Dr. Colin Burns, Ph.D.

COMMITTEE MEMBER: _____
Dr. Yu Yang, Ph.D.

COMMITTEE MEMBER: _____
Dr. Paul Hager, Ph.D.

CHAIR OF THE DEPARTMENT
OF CHEMISTRY: _____
Dr. Andrew Morehead, Ph.D.

DEAN OF THE
GRADUATE SCHOOL: _____
Dr. Paul J. Gemperline, Ph.D.

I thank God for giving me the power and strength to go through life with a smile and allow me to pursue a higher calling and education

Surah Taha 20: 114

This thesis is dedicated to my family whose love and prayers have guided me to each at this point in life. I will continue to work for them.

ACKNOWLEDGEMENTS

I would like to express my gratitude and appreciation to my advisor, Dr. Robert Hughes, for his guidance. He gave me an opportunity to be the first on his team and help build his lab. It was an honor to be his first graduate student at East Carolina University. I will never forget what he has given me during my years here as a master's student.

I give my thanks to the Department of Chemistry for giving me not only financial help but the opportunity to grow as a person. I became more than a chemist here; I became a better person and a man here. For that, I give all my love and support to this great department.

I wish to give thanks to all my friends and fellow graduate students: Katie Vang, Tori Angermeier, Fatema Salem, Eshitha Karnik, Erman Javed, Tyler Israel, Cheyenne Bowman, Katherine Buddo and Jennifer Marechek. They have given more than friendship, and it will be hard to repay.

TABLE OF CONTENTS

LIST OF TABLES

LIST OF FIGURES

LIST OF ABBREVIATIONS

AD	Alzheimer's Disease
NDD	Neurodegenerative diseases
ATP	Adenosine triphosphate
ADP	Adenosine diphosphate
APP	Amyloid precursor protein
DISC	Death-inducing signaling complex
DNA	Deoxyribonucleic acid
ROS	Reactive Oxygen Species
Aβ	Amyloid Beta
kDa	Kilodalton
aa	Amino acids
ABP	Actin-binding protein
ADF	Actin depolymerizing factor
DSC	Differential scanning calorimetry
Tm	Melting Temperature
Cry2	Cryptochrome
SDS	Sodium dodecyl sulfate
PAGE	Polyacrylamide gel electrophoresis
CD	Circular Dichroism
min	Minute
MALDI	Matrix assisted laser desorption ionization
TOF	Time-of-flight
PCR	Polymerase chain reaction

CHAPTER 1: INTRODUCTION

A number of neurodegenerative diseases are accompanied by the formation of cofilin-actin rods in neural cells. These rods can cause synaptic dysfunction and block transport within neurites (1). The overall goal of this project is to create an optogenetic switch that incorporates both cofilin (an actin-binding protein) and actin for the study of cofilin-actin rod formation in neural cells undergoing oxidative stress.

To accomplish this, we first need to develop an actin mutant with altered nucleotide binding affinities for ATP and ADP. In order to achieve this goal, we will pursue the following aims: (i) Develop a robust expression and purification protocol for β-actin; (ii) Develop an assay for actin-nucleotide binding based on literature precedent; (iii) Create actin mutants designed to have different affinities for ATP and ADP and study them by spectroscopic and calorimetric methods; (iv) incorporate the actin mutants into optogenetic constructs.

1.1 Neurodegenerative Diseases

Neurodegenerative diseases are characterized by progressive neurological dysfunctions that are associated with neuron cell death in the nervous system (2). Efforts have been focused on defining the pathways, both cellular and molecular. There are numerous different forms of neurodegeneration, and each involves different proteins, with amyloid beta being one of the most highly studied. Defective cellular processes lead to amyloid beta (Aβ) forming oligomers which are directly connected to synaptic damage in neurons (3). Furthermore, the effects of mutations in proteins such as APP, tau, and presenilin-1 on protein oligomerization have been investigated (3). Abnormal activation of signaling pathways that contain these proteins can also lead to synaptic failure. Further investigation of these pathways may lead to the discovery of ways to stop or slow down the development of neurodegenerative diseases.

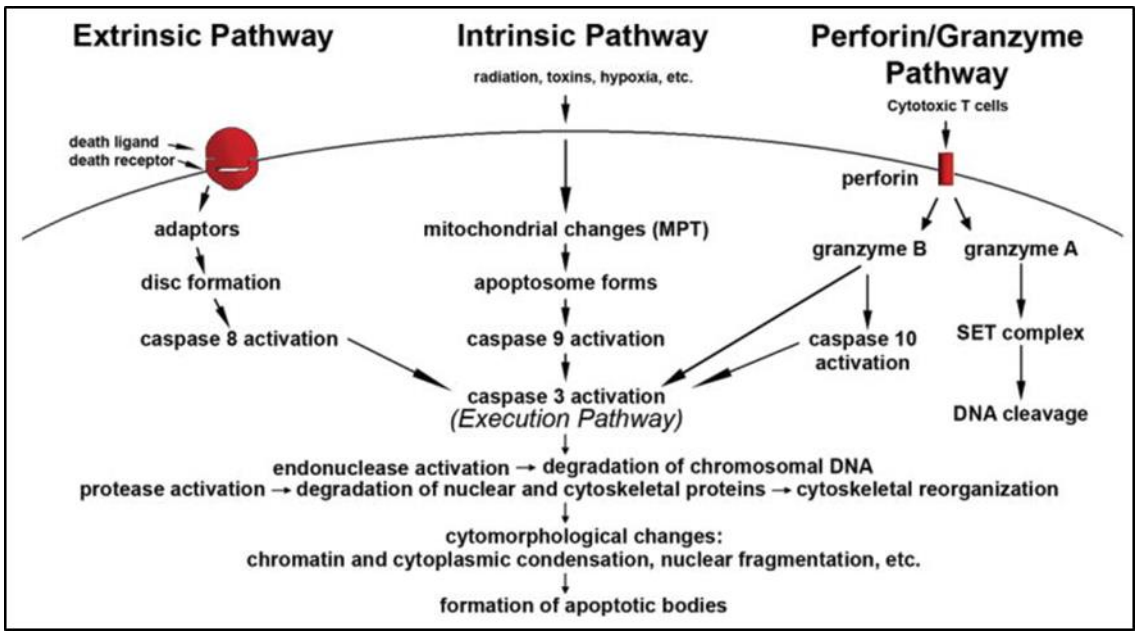

Figure 1.1 Apoptosis Pathway. *Used by permission from "Knopman D. Clinical Aspects of Alzheimer's Disease. In: Neurodegeneration: The Molecular Pathology of Dementia and Movement Disorders. Wiley-Blackwell; 2011. p. 37-50 "The two main pathways of apoptosis are extrinsic and intrinsic as well as a perforin/granzyme pathway. Each requires specific triggering signals to begin an energy-dependent cascade of molecular events. Each pathway activates its own initiator caspase (8, 9, 10) which in turn will activate the executioner caspase-3. However, granzyme A works in a caspase-independent fashion. The execution pathway results in characteristic cytomorphological features including cell shrinkage, chromatin condensation, formation of cytoplasmic blebs and apoptotic bodies and finally phagocytosis of the apoptotic bodies by adjacent parenchymal cells, neoplastic cells or macrophages.*

The culmination of neurodegenerative disease progression is cell death. There are two morphological types of cell death: apoptosis and necrosis. Apoptosis is programmed cell death that occurs in multicellular organisms. Apoptosis regulates the cell population and is activated by extrinsic or intrinsic pathways (4). Both types of pathways activate protease enzymes (caspases) which initiate the execution pathway of cell death (Figure 1.1). During the extrinsic pathway, the caspase is activated by extracellular ligands via cell surface receptors. This occurs by the formation of a multiprotein complex, dubbed death-inducing signaling complex (DISC), that recruits and activates a pro-caspase (5). The intrinsic pathway does not involve external receptors but proceeds during times of cellular stress. During apoptosis, the mitochondrial outer membrane is permeablized. As a result, mitochondrial cytochrome c is released into the cytosol. This molecule binds an adaptor protein which recruits an initiator caspase, leading to the formation of a caspase-activating multiprotein complex called the apoptosome. Once activated, initiator caspases will

Table 1.1 Morphological features of apoptosis and necrosis Table

Apoptosis	Necrosis
Single Cells or small clusters of cells	Often contiguous cells
Cell Shrinkage and Convolution	Cell swelling
Pyknosis and Karyorrhexis	Karyolysis, pyknosis, and karyorrhexis
Intact cell membrane	Disrupted cell membrane
Cytoplasm retained in apoptotic bodies	Cytoplasm released
No inflammation	Inflammation usually present

Table 1.1 Morphological features of apoptosis and necrosis *Table was adapted from "Elmore S. Apoptosis: A Review of Programmed Cell Death. Toxicologic Pathology. 2007 Jun;35(4):495-516." Comparison of morphological features of apoptosis and necrosis*

cleave and activate other executioner caspases. The caspases lead to degradation of cellular components for apoptosis. In the final stages of apoptosis, the cytoskeletal proteins and DNA are degraded, leading to nuclear fragmentation, degradation of subcellular components, the collapse of the cytoskeleton, the formation of apoptotic bodies, and ultimately clearance of the cellular remains in vivo (6).

Unlike apoptosis, which is a natural phenomenon that maintains the cell population, necrosis is not programmed and causes several side effects such as inflammation and cell damage (Table 1.1). Necrosis affects surrounding cells and tissue, whereas apoptosis does not (6). In apoptosis, there are no inflammatory reactions because apoptotic cells do not release their contents into the surrounding areas and their cellular constituents are quickly phagocytosed by the surroundings cells; in theory, this prevents secondary necrosis (Table 1.1). Also in apoptosis, the engulfing cells do not produce any other cytokines that result in anti-inflammatory actions, which prevents further surrounding cell damage (7).

1.1.1 Oxidative Stress

Oxidative stress occurs when free radicals and their products are more abundant than antioxidant levels (8). Free radicals are atoms, molecules, or ions that have an unpaired valence electron and are very reactive. Antioxidants maintain the balance of free radicals, which can

Table 1.2 Major endogenous oxidants.

Oxidant	Formula	Reaction Equation
Superoxide Anion	$O_2^{-\cdot}$	$NADPH + 2O_2 \leftrightarrow NADP^- + 2O_2^{-\cdot} + H^+$ $2O_2^{-\cdot} + H^+ \rightarrow O_2 + H_2O_2$
Hydrogen Peroxide	H_2O_2	$Hypoxanthine + H_2O + O_2 \rightleftharpoons Xanthine + H_2($ $Xanthine + H_2O + O_2 \rightleftharpoons Uric\ Acid + H_2O$
Hydroxyl radical	$\bullet OH$	$Fe^{2+} + H_2O_2 \rightarrow Fe^{3+} + OH^- + \bullet OH$
Hypochlorous acid	$HOCl$	$H_2O_2 + Cl^- \rightarrow HOCl + H_2O$
Peroxyl radicals	$ROO^\bullet$	$R^\bullet + O_2 \rightarrow ROO^\bullet$
Hydroperoxyl radical	$HOO\cdot$	$O_2^- + H_2O \rightleftharpoons HOO\cdot + OH^-$

Table adapted from Birben et al. Oxidative stress and antioxidant defense. The World Allergy Organization journal. 2012 Jan;5(1):9-19.

change and alter cells and cellular functions. Reactive oxygen species (ROS) are byproduct radicals that are produced by metabolic pathways such as glycolysis (8).

The endogenous sources of ROS that play the most significant role in cellular stress are superoxide anion (O_2^-), hydroxyl radical (●OH) and hydrogen peroxide (H_2O_2) (Table 1.2). Superoxide anions are formed by the addition of 1 electron to the molecular oxygen. This process is mediated by nicotine adenine dinucleotide phosphate (NADPH) oxidase or xanthine oxidase or by mitochondrial electron transport system. The primary site for producing superoxide anion is the mitochondria. Typically, electrons are transferred through mitochondrial electron transport chain for reduction of oxygen to water, but approximately 1 to 3% of all electrons leak from the system and produce superoxide (9).

Hydrogen peroxide is also produced by xanthine oxidase, amino acid oxidase, and NADPH oxidase and in peroxisomes by consumption of molecular oxygen in metabolic reactions. O_2^- itself can even react with H_2O_2 and generate $^\bullet$OH. Hydroxyl radical is the most reactive ROS (8).

Cigarette smoke contains many free radicals and is one common source of exogenous ROS. Furthermore, heavy ions like iron, copper, mercury, arsenic, lead, cadmium, and nickel can

generate radicals which cause cellular damage via depletion of enzymatic activity (8). Humans have natural defenses against ROS and other radicals. For example, the enzyme superoxide dismutase (SOD), catalyzes the dismutation of superoxide into oxygen or hydrogen peroxides (10). Vitamins such as Vitamin A can be found in whole milk and vegetables, and they can neutralize radicals by donating an electron to reduce these radicals.

There have been many studies that show that oxidative stress, radicals, and ROS are part of the pathogenesis of neural degeneration in NDD and AD. One of the most extensive studies was performed at the Sander-Brown Center of Aging and Alzheimer's at the University of Kentucky Medical Center. This study focused on the link between that oxidative stress and the pathogenesis of neuron degeneration, using oxidative-sensitives enzymes as markers for oxidative species in certain cells in the presence of external oxidants (11).

1.1.2 Alzheimer's disease

Alzheimer's disease (AD) is the most common cause of dementia, which is a syndrome that results in cognitive decline and impairment (12). Dementia is assessed as interference with the ability to function in normal activities and a reduction from prior levels of functioning and performing (9). Another way to diagnose and detect cognitive impairment is through objective cognitive assessment. Cognitive impairments include impaired ability to acquire and remember new information, impaired reasoning and handling of a complex task, poor judgment, impaired visuospatial abilities, and changes in personality, behavior or comportment (2).

Alzheimer's occurs in stages and progresses more rapidly during the middle to late years of life. A definite diagnosis of Alzheimer's disease requires a histopathologic confirmation. However, studying brain tissue can only take place after a person is deceased. A clinical diagnosis

is never definite and could be misdiagnosis as Parkinson's or any other NDD. There is a lengthy diagnosis process that includes: acquisition of medical history, neurologic examinations, psychiatric examinations, clinical examinations, neuropsychological test and laboratory studies (12).

The biochemistry of AD is characterized by the accumulation of Aβ peptide in the functioning part of the brain (Parenchyma) and also by the accumulation of the tau protein in neurofibrillary tangles (13). The Aβ peptide comes from the protein amyloid precursor protein (APP) which is responsible for signal transduction. Cleavage of Aβ from APP forms a soluble, 39-42 amino acid long peptide with a helical structure (13). However, misfolding of the peptide can occur, resulting in the formation of β-sheet structures and subsequent aggregation. The resulting rod-like structures, called fibrils, are highly insoluble and thermodynamically stable and structurally organized.

Amyloid plaques found in AD patients and in murine brains represent the final state of the aggregation process *in vivo*. They are large extracellular deposits composed of insoluble amyloid fibrils and intimately surrounded by dystrophic dendrites, axons, activated microglia, and reactive astrocytes. These can cause physical changes to the brain (13).

ROS and oxidative stress is part of the pathology of AD and other neurodegenerative diseases. Aβ binds to metal ions, and the formation of complexes with these metals can generate ROS such as H_2O_2 (14). Neurons displaying signs of oxidative stress are not necessarily succumbing to oxidative stress but adapting by way of oxidant defenses (15).

1.2 Actin

Actin is a protein often associated with muscle cell function but is also involved in numerous other processes. Actin is one of the abundant protein in eukaryotic cells (16). The protein is located throughout the cell, including the cytoplasm and nucleus while giving the cell structure. Actin is also highly conserved, with a highly similar amino acid sequence across species (17).

Actin was first isolated in 1943 in Hungary at the University of Szeged in the Laboratory of Albert Szent-Gyorgyi by Bruno Straub. It was not until after World War II that he was given credit for the discovery (18). Some years earlier (in 1859), Wilhelm Friedrich Kühne reported that he had found the component necessary for muscle contraction from a frog muscle (19). Today, we know this component as the actomyosin complex.

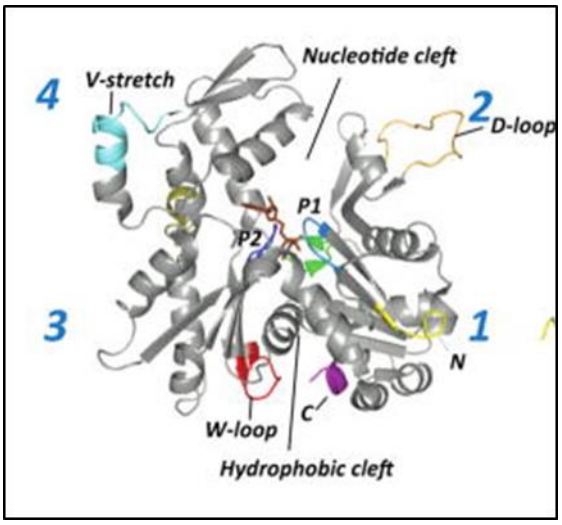

Figure 1.2 Actin Ribbon Structure *Used by permission from "Kudryashov DS, Reisler E. ATP and ADP actin states. Biopolymers. 2013 Apr;99(4):245-56" G-actin Structure. The flexible segments of actin are colored as follows: the phosphate binding loops P1 (a.a. 11–16) and P2 (a.a. 154–161) are in light and dark blue, respectively; the sensor loop (a.a. 70–78) is in green; the H-plug (a.a. 264–271) is in olive; the D-loop (a.a. 40–51) is in orange; the W-loop (a.a. 165–172) is in red; the V-stretch (a.a. 227–237) is in cyan; the N- and C-terminal regions are colored in yellow and purple, respectively.*

Actin has two forms: monomeric (G-actin) and filamentous (F-actin). Actin is a globular protein with three different isomers: α, β, and γ. α-actin is responsible for muscle contractions and is found in skeletal, smooth, and cardiac muscle cells. β- and γ-actin is found in the cytoplasm of cells and are part of the cytoskeleton of all cells and plays roles in cell division, moiety, morphogenesis and organelle positions (16).

Actin is 375 amino acids long and has a molecular weight of approximately 42 kDa. Actin has a globular shape with two major domains, a larger inner domain, and a smaller outer domain. The two domains are further divided into subdomains SD 1-4 (20). Nucleotides are bound in a cleft between SD 2 and 4 (binding cleft) in phosphate binding loops (P1 and P2) amino acid

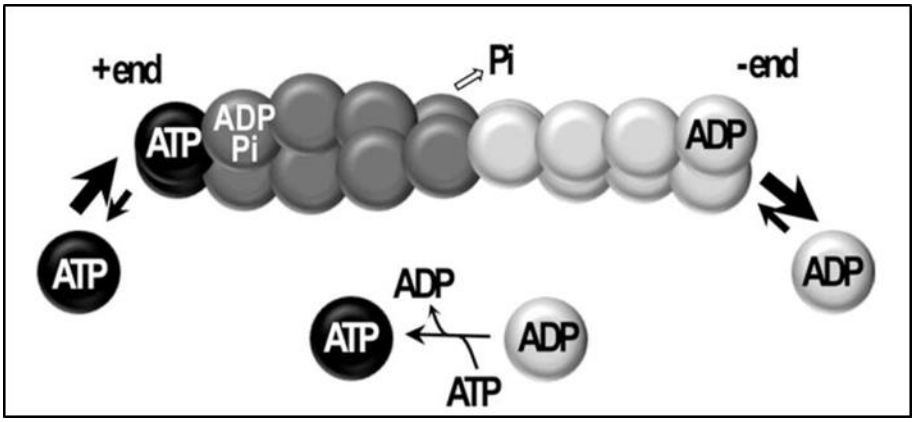

Figure 1.3 Actin Treadmilling *Used by permission from Kudryashov DS, Reisler E. ATP and ADP actin states. Biopolymers. 2013 Apr;99(4):245-56" Schematic representation of actin treadmilling: Under steady state conditions in the presence of ATP, actin protomers containing ADP dissociate predominantly from the minus end of the filament, exchange the nucleotide in the cleft from ADP to ATP, and then ATP-containing protomers associate predominantly at the plus end of the filament. The dissociation from the minus end is potentiated by cofilin; ADP to ATP exchange is promoted in solution by profilin. Both proteins sense nucleotide-dependent conformations of actin. Overall, ATP hydrolysis by filamentous actin fuels the translocation of protomers from one end of the filament to the other.*

residues 11-16 and 154-161. There is a 2nd cleft opposite of the Nucleotide cleft called the hydrophobic cleft where actin-binding proteins can bind (20) (Figure 1.2). β-actin is an ATPase and can bind to adenosine triphosphate (ATP) or adenosine diphosphate (ADP). Both nucleotides are key to the formation of filament actin (F-actin). ATP is essential for monomer stability.

The structural differences between the ATP and ADP bound states of actin are fairly minimal. The primary difference occurs between the two loops at Ser14 and His73. These loops engulf the phosphates of the nucleotide (21). Ser 14 binds to the terminal phosphate of ATP. After hydrolysis and release of the terminal phosphate, Ser14 changes orientation to form a hydrogen-bonding contact with the β-phosphate, while the His73 loop moves toward the nucleotide to take up the space that was occupied by the terminal phosphate (21).

F-actin filaments are created from G-actin bound to ATP. In a process called treadmilling, they start to assemble into dimers and trimers and form stable oligomers before incorporating into filaments (Figure 1.3) (16). ATP/G-actin complexes assemble at the barbed end of the filament, while ADP/G-actin complexes dissociate from the pointed end.

F-actin is the most abundant form of actin. Non-muscle F-actins are organized into bundles that are found in the plasma membrane like microvilli or filopodia (18). F-actin fulfills cytoskeletal functions such as cell stabilization and the formation of membrane extensions (19).

1.2.1 Actin-Binding Proteins

As previously discussed, actin remodeling is responsible for cell movement (17). Actin filaments are part of the cytoskeleton and can form high order structures or actin networks. The actin cytoskeleton is highly regulated at different levels by several proteins called Actin-Binding Proteins (ABPs). There have been over 160 different actin-binding proteins (ABPs) identified which are involved in the assembly of F-actin or the organization of F-actin filaments (18).

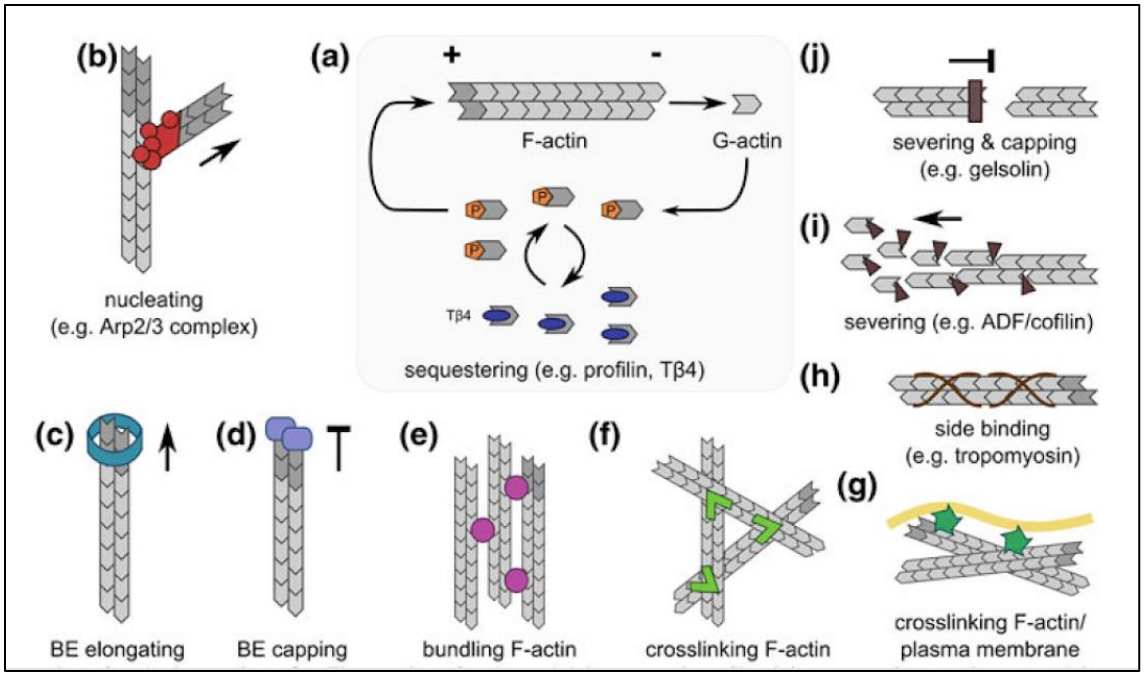

Figure 1.4 Types of Actin Binding and functions *Used by permission from "Mannherz HG. The actin cytoskeleton and bacterial infection. Cham, Switzerland: Springer; 2017" The effects of the diverse classes of actin-binding proteins (ABPs) on actin dynamics a) F-actin in equilibrium with G-actin that can be sequestered by binding to profilin. B-J) is the effects of difference ABP types on F-actin.*

Most ABPs induce the formation of F-actin to make the formation easier or to regulate the polymerization of F-actin by decreasing the activation energy of treadmilling either by severing or depolymerizing. F-actin can be manipulated in many ways, such as increasing the barbed end elongation rate, preventing the assembly of additional G-actin promoters, and by disassembling F-

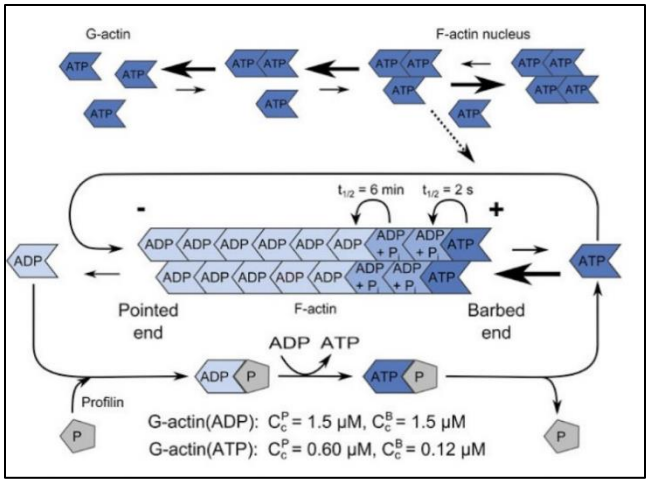

Figure 1.5 Nucleation and polymerization process of F-actin*. Used by permission from "Mannherz HG. The actin cytoskeleton and bacterial infection. Cham, Switzerland: Springer; 2017" The formation of nuclei from ATP-actin molecules and the cyclic scheme the process to F-actin.*

actin by binding and severing. There are many diverse classes of ABPs with actin dynamics ranging from the capping to the severing of F-actin (Figure 1.4).

Treadmilling is powered by the ABP Profilin. Profilin enhances the ADP exchange of G-actin that makes ATP-G-actin (Figure 1.5). Profilin interacts with actin by binding to the binding site of actin found in between subdomain I and III (Figure 1.2). Profilin enhances the process of treadmilling by speeding up the barbed end process of polymerization and elongation. While there are other ABPs that assist in the same process, such as β-thymosin, profilin has a greater binding affinity for G-actin and may be the primary facilitator of G-actin nucleotide exchange.

The Arp2/3 complex plays a role in the regulation of actin filaments and the actin cytoskeleton. It starts a side branch filament onto a "mother" filament which initiates a branched actin network. The complex acts as a capping protein at the pointed end that encourages rapid growth from the barbed end (22).

Severing ABPs are the most important of actin-binding proteins because they maintain the length of F-actin and the polymerization rate. Two well-characterized severing proteins are Gelsolin and ADF/Cofilin. They are responsible for the breakdown of straight or branched actin filaments.

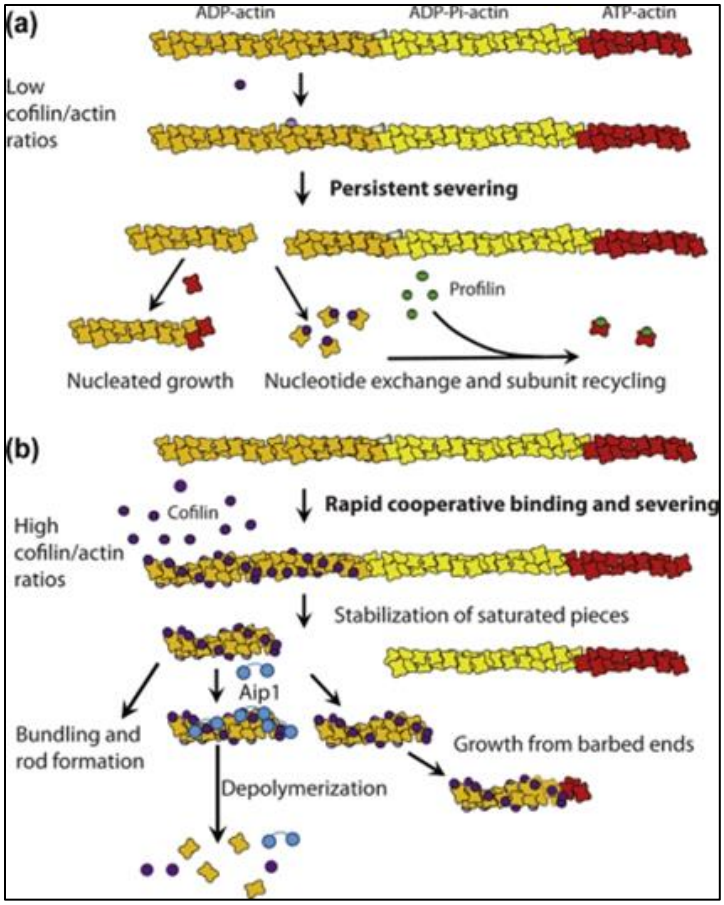

Figure 1.6 Concentration effects of cofilin on actin dynamics *Used by permission from Bamburg JR, Bernstein BW. Roles of ADF/cofilin in actin polymerization and beyond* ***(a)*** *Cofilin (purple) binds preferentially to ADP-actin (orange) and, at low stoichiometry with respect to actin subunits, severs filaments, creating new barbed and pointed ends. The cofilin dissociates with an actin subunit in the ADP form, and nucleotide exchange* ***(b)*** *At higher stoichiometry, cofilin binds to ADP-actin, but since binding is cooperative, regions of the F-actin become saturated and stabilized in the 'twisted form'. Severing occurs rapidly, but as the cofilin is sequestered on the pieces of actin, severing is not persistent. Fragments are further depolymerized in the presence of actin-interacting protein 1 (Aip1) (blue) to generate monomer or can be used to nucleate growth. In cells under stress where ADP-actin levels are elevated, the cofilin-saturated F-actin assembles into rod-shaped bundles.*

Cofilin represents a family of proteins, including Cofilin 1 (non-muscle), Cofilin 2 (muscle), and Destrin or actin depolymerizing factor (ADF). Whether cofilin promotes actin assembly/disassembly depends upon the relative concentration of actin and other actin-binding proteins present in the cell (16). When the concentration of actin and cofilin are high enough actin bundles (rods), start to form.

Cofilin is regulated through very complex dynamics and extracellular signaling. Cofilin is deactivated by phosphorylation on Ser3 which inhibits actin binding. This is done by several kinases, such as LIM kinase, which have several downstream activations (23). The dephosphorization of cofilin can be regulated by the availability of the Ser3 phosphate to phosphatase activity by a specific phosphatase called Slingshot. This recently identified protein functions both in vivo and in vitro to dephosphorylate ADF/cofilin (23). However, upstream regulators of slingshot have not yet been reported (24).

1.2.2 ADF/cofilin Actin Rods

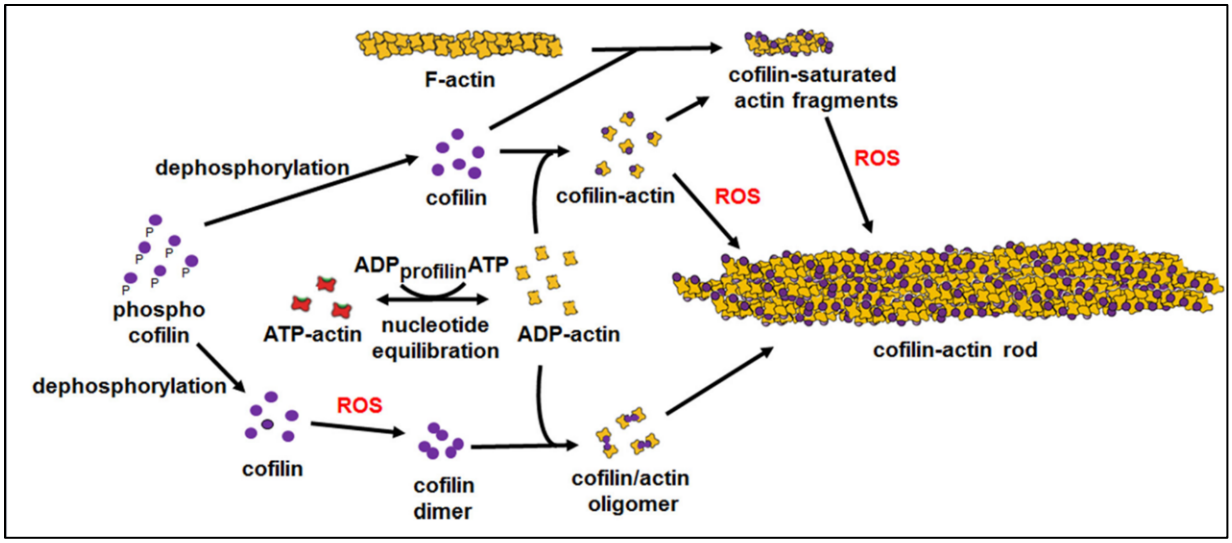

Figure 1.7 Cofilin-actin rod formation. *Used by permission from Bamburg JR, Bernstein BW. Actin dynamics and cofilin-actin rods in Alzheimer disease. Cytoskeleton. 2016;73(9):477-97.Pathways to Rod formation. Oxidative cross-linking of cofilin before and after binding to F-actin to actin monomers to induce rod assembly. Profilin Binding to actin monomers opens the nucleotide pocket allowing the actin-bound nucleotide to equilibrate with the cellular adenine nucleotide pool.*

Activated cofilin (dephosphorylated at Ser3) saturates actin filaments causing them to bundle into rod structures (Figure 1.6). These rods can cause synaptic dysfunction and blocks transport within neurites. This occurs in either the nucleus or cytoplasm which halts actin polymerization and thus freeing ATP (16). In stressed cells, the level of ATP decreases and oxidation potential increases which effects cofilin activity, increasing the likelihood of cofilin-actin rod formation. Also, during cellular stress, glycolysis is inhibited which increases ADP concentration. Importantly, these rods dissociate quickly following relief of the transient stress (Figure 1.7) (16).

1.3 Previous Studies

Previous studies have been performed to investigate the dynamics of actin structure and binding. Differential scanning calorimetry (DSC) was used to monitor the thermal stability of actin-binding proteins to actin. This study characterizes and compares the effects of cofilin, twinfilin, and profilin on the unfolding of monomer actin when binding to ATP or ADP. The results

showed that actin thermal stability depends on the identity of the bound nucleotide (25). Cofilin binding stabilizes both ATP-actin and ADP actin while another ABPs stabilizes either ATP or ADP-Actin. This DSC study, done by Pivovarova and her group at the Russian Academy of Sciences, provides valuable info about conformation changes of nucleotide binding (Figure 1.8) (25).

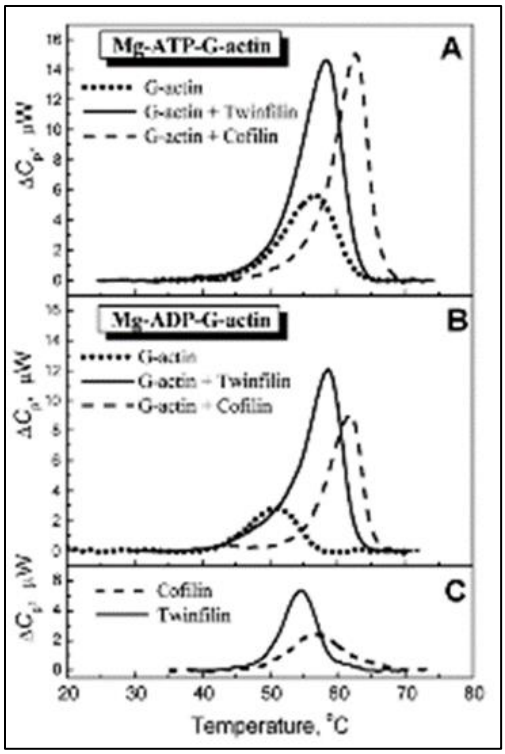

Figure 1.8 Nucleotide Binding of Actin and Temp Dependence *Used by permission from Pivovarova AV, Chebotareva NA, Kremneva EV, Lappalainen P, Levitsky DI. Effects of actin-binding proteins on the thermal stability of monomeric actin. Biochemistry. 2013 January;52(1):152-60 Temperature dependencies of the excess heat capacity (ΔCp) of ATP−Mg−G-actin (A) and ADP−Mg−G-actin (B) in the absence and presence of cofilin-1 or twinfilin-1. The concentration of actin was constant (15 μM), and the molar concentrations of cofilin and twinfilin in the complexes were 15 μM. (C) DSC curves of cofilin (15 μM) and twinfilin (15 μM) in the absence of actin. The heating rate was 1 K/min.*

Another study has used TNP-ATP (εATP). εATP is a fluorescent molecule that can determine whether a protein binds to ATP and the constants associated with that binding. It has a fluorescent probe which can be used in fluorescence spectroscopy and x-ray crystallography. Kinosian and his group at Albany medical college found the dissociation rates of ADP and ATP from actin by displacing bound nucleotide with large amounts of εATP. The time course of the fluorescent intensity increase upon binding to actin and a program to determine the dissociation rate constant (26).

One other study shows that the loss of DNase I-inhibition activity of actin at increased temperature was correlated with the thermal unfolding of actin. The DNase-1 inhibition assay is a simple assay for the quantification of kinetic parameters for the irreversible denaturating of G-actin. The results show that actin isoforms differ in thermal stability and that the stability of actin depends on the nature of the bound nucleotide. In addition, a thermal

melting curve was found that showed a correlation of unfolding to the temperature (27) and the melting temperature (Tm) was taken of DNase-1.

1.4 Goals/Methodology

The overall goal of this project is to create an optogenetic switch to control the formation of cofilin-actin rods. This project focuses on the nucleotide equilibrium and the nucleotide binding of actin. The first step in this project was the protein expression of β-actin. After establishing a protocol for the expression and purification of native actin, we then conducted site-directed mutagenesis, a technique that changes amino acid sequences by introducing mutations to the parent gene. Eight mutations were attempted, and residue changes were based on the 3D crystal structure of the nucleotide cleft of β-actin. Next, we attempted a spectroscopic assay that could test and analyze nucleotides binding of the expressed protein. Finally, we created an optogenetic actin construct, utilizing the light responsive dimerizer proteins Cryptochrome 2 and Cib. This light-activated dimerized system is activated by blue light (488 nm) and fused, respectively, to cofilin and β-actin (28).

1.4.1 SDS-PAGE

One of the many techniques we used to characterize our expressed protein will be an SDS-PAGE. This technique is used to separate biomolecules based on their molecular weight and electric charge. Electrophoresis has many applications. For example, it is used in DNA fingerprinting and detection of genetic variants. It is also used for the detection of pathogens that may be found in blood or other tissues (29).

A few proteins like tubulin do not bind at this ratio, and this is one reason why some proteins migrate anomalously (31). Since SDS is an anionic detergent, it imparts a negative charge to all the proteins in the sample. More importantly, these charges swamp the inherent charge of

the proteins and give every protein the same charge-to-mass ratio. Because the proteins have the same charge-to-mass ratio, and because the gels have sieving properties, mobility becomes a function of molecular weight (31).

1.4.2 Circular dichroism

Circular dichroism (CD) is a spectroscopic method for evaluating secondary structure, folding and binding properties of proteins. CD is the absorption of left and right-handed circularly polarized light. If the light is polarized by passing the beam through a suitable prism or filters, its electric field, E, will oscillate in a single plane. CD is reported in units of molar ellipticity (ΔE) (32).

Structural changes in proteins caused by the binding of ligands are an essential part of the mechanism of action and regulation of biological activity. CD provides an experimentally convenient means of detecting such changes which can be examined in different spectral regions In addition, CD can be used to assess the range of ligand concentrations over which structural changes take place, the extent of the changes in the protein of interest and (using time-resolved CD studies) the speed at which such changes occur. CD is especially invaluable in the study of peptides where X-ray crystallography is not generally practical (33).

1.4.3 Mass Spectrometry

Mass Spectrometry will be used to confirm the mass of the expressed protein. Mass spectrometry has become a widely used tool for protein sequencing and fingerprinting (34). This is largely due to the introduction of soft ionization sources for analysis of biomolecules, such as electrospray ionization and matrix-assisted laser desorption ionization. Combined with time-of-flight (TOF) it creates a technique that makes it easier to find the weight of expressed protein.

In MALDI, the sample is mixed with a matrix, and a droplet of the mixture is spotted on a plate and allowed to dry. The plate is hit with a very short pulse of light from a laser. Matrix molecules absorb energy from the incident light; this energy is used to volatilize the sample and transfer protons from the matrix to molecules in the sample, instantaneously forming a group of ions. This ionization method favors the production of ions having a single charge (35).

The ions formed are accelerated into the source region of a TOF mass spectrometer. At intervals, a high voltage pulse is used to send ions into the flight tube (a field-free region), where they separate according to kinetic energies. The kinetic energy (KE) associated with a given ion can be expressed in two ways: with respect to the potential applied or with respect to the resulting velocity of ions (34). TOF is usually used in conjunction with MALDI because of its large mass range. One of the benefits of MALDI/TOF is that it tends to keep the protein intact, while other techniques fragment the protein, making the analysis more complicated.

1.4.4 Protein Expression

Protein Expression is a technique that enables large-scale production of proteins. In bacterial protein overexpression, plasmid DNA is transformed into a bacterial host strain such as BL-21. We created recombinant protein by taking the gene of interest and cloning it in an expression vector, transform it into a host cell, induce and finally purification (36). The first step involves the design of specific gene PCR amplification primers, followed by a screening of potential PCR-amplified clones for proper insert orientation. Sequence analysis of positive clones must be performed, to confirm that a proper reading frame has been obtained and that no PCR-introduced errors are present (37).

Affinity tags are commonly used in protein expression. N- and C-terminal expression tags are used in expression vectors to help with purification to increase protein recovery by fusing to

the protein of interest and used to expedite protein purification via affinity chromatography. 6X His repeat tags have strong interactions with transition metal ions, such as Ni^{2+} and Co^{2+} (37). Histidine is the amino acid that exhibits the strongest interaction with immobilized metal ion matrices, as electron donor groups on the histidine imidazole ring readily form coordination bonds with the immobilized transition metal. Peptides containing sequences of consecutive histidine residues are efficiently retained on IMAC column matrices. Following washing of the matrix material, peptides containing poly-histidine sequences can be easily eluted with imidazole thus increasing recovery of the target protein (38).

The primary goal of bacterial overexpression of actin is to isolate the required quantity of β-actin in its active form. Soluble proteins can be recovered with good yields (>50%), and insoluble proteins, which must undergo denaturation and folding cycle, can be recovered with more modest yields (5% to 20%). (39) Due to low quantities of soluble protein in our experimental trials, we decided to pursue isolation of actin from inclusion bodies.

Inclusion bodies are protein aggregates of a target protein that form during overexpression. Inclusion bodies are normally formed in the cytoplasm (Figure 1.10). If a secretion vector is used, they can form in the periplasmic space. Inclusion bodies are not restricted to E. coli; they can also form in yeast, mammalian, and insect cells. Inclusion bodies recovered from cell lysates by low-speed centrifugation are heavily contaminated with E. coli cell wall and outer membrane components (40).

Protocol: Inclusion body prep of β-actin. We started with a plasmid pNic-28 encoding a gene for β-actin which were later transformed into BL-21(DE3) and plated onto LB-Kan agar plates. We picked a single colony from the agar plate and used it to inoculate a 30 mL terrific broth culture which was grown overnight with shaking (200 rpm) at 30 °C. The next day we took 10 mL

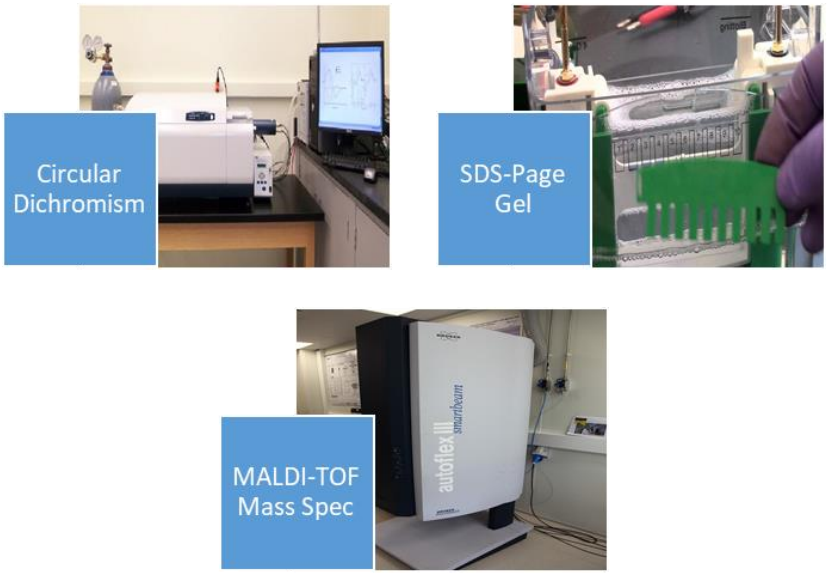

Figure 1.9 Experimental techniques*. Circular Dichroism will monitor secondary structure and folding of the protein. SDS-Page will be used to analyze protein expression and purification.. MALDI will be used to confirm molecular weight of proteins that are expressed.*

of the culture and used that to inoculate 200 mL of LB-Kan media. The media was grown to mid-log phase (37 °C; 200 rpm) than 1 mM of IPTG was added to the culture which was later incubated overnight at 20 °C.

The culture was centrifuged at 5000 rpm, and 4 °C and the supernatant was discarded. The pellet that left was then lysed using 10 mL B-PER/1X protease inhibitors. The resulting culture was centrifuged for 20 mins (14000 rpm) at 4 °C where the supernatant and pellet were kept in the -80 °C freezer. The supernatant was put thru a gravity column containing HisPur Cobalt resin. This was performed two times. The column was washed with wash buffer (2x 10 mL; 20 mM imidazole buffer) and then eluted with 1 M imidazole. The lysed (soluble) fraction was then analyzed by SDS-PAGE.

The frozen pellet (insoluble fraction) was thawed and resuspended in 10 mL B-PER, and 40 µL of lysozyme (200 µL of a 10 mg/mL stock; 50% glycerol solution) was added. The solution was then mixed well and incubated for 5 min at room temperature. Finally, 100 mL of 1:10 diluted B-PER reagent was added to the solution and vortexed.

The inclusion bodies were harvested by centrifugation (15 min; 14000 rpm). The resulting pellets were resuspended in 100 mL 1:10 diluted B-PER reagent. Solutions were then sonicated on ice to reduce clumping, and this was done twice. The remaining solution which contained the

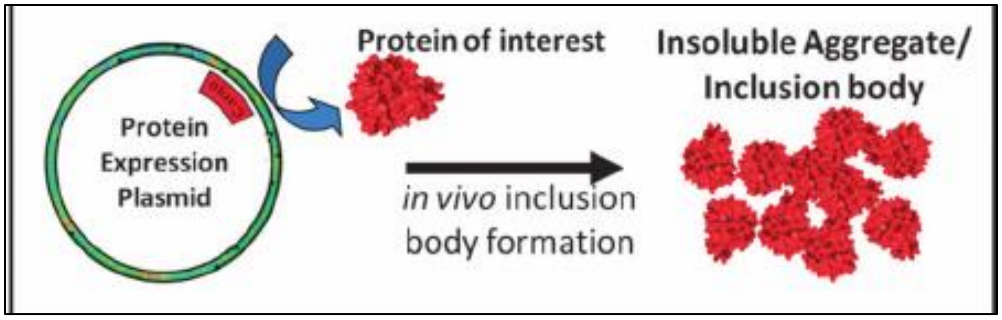

Figure 1.10 Inclusion body formation *Adapted from Patterson, Dustin & Lafrance, Benjamin & Douglas, Trevor. (2013). Rescuing Recombinant Proteins by Sequestration Into the P22 VLP. Chemical communications (Cambridge, England). 49. 10.1039/c3cc46517a. The probability of successfully expressing a soluble protein decreases considerably at molecular weights above ~60 kDa. Proteins that do not express in soluble form may not be modified or folded properly, or may precipitate within E. coli through formation of inclusion bodies*

inclusion bodies were solubilized in 5 mL of 50 mM Hepes (pH 7.5)/6 M Guanidinium HCl/25 mM DTT and incubated at 4 °C for 1 h, then centrifuged (14000 rpm; 10 min; 4 °C) to remove any remaining insoluble material. The concentration was determined by a Bradford assay.

The protein was diluted to 1 mg/mL in HEPES solubilization buffer and then diluted once more into refolding buffer (5 mL sample into 45 mL refolding buffer; 50 mM glycine (pH 9)/200 mM NaCl/5 mM EDTA/10 mM DTT/1X protease inhibitors) on ice. The resulting solution was mixed vigorously for 2 min. Lastly, the sample was spin concentrated, dialyzed via snake dialysis tubing at 4 °C overnight in 2 L of 1X Tris-buffered saline (Figure 1.11). The sample was later analyzed by western blot.

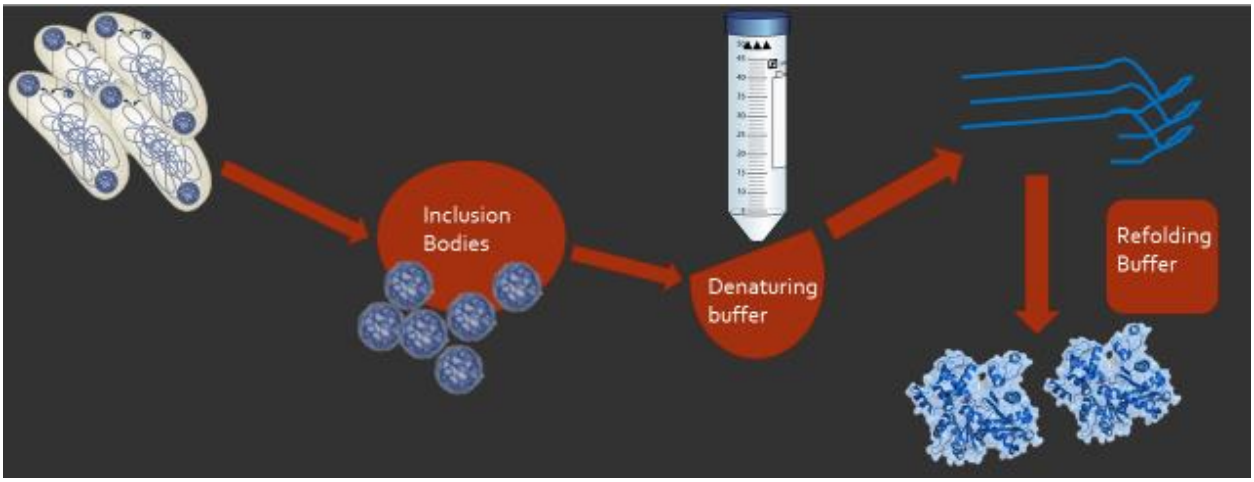

Figure 1.11 Inclusion Body preparation protocol*: (1) E coli Cells are lysed, (2) the cell wall and outer membrane components are removed, (3) the aggregates are solubilized (or extracted) with strong protein denaturants, and (4) the solubilized, denatured proteins are folded with concomitant oxidation of reduced cysteine residues into the correct disulfide bonds to obtain the native protein.*

1.4.5 Mutagenesis

We want to investigate the binding site of G-actin to nucleotide(s) and how this connects with cofilin-actin rod formation (20). By altering the nucleotide binding site of actin to change nucleotide affinity, we may gain a greater understanding of cofilin-actin rod formation. To accomplish this goal, we used site-directed mutagenesis to introduce point mutations into the nucleotide binding pocket of β-actin.

Site-directed mutagenesis is a method used to make changes to DNA sequences of a gene. A single amino acid change by site-directed mutagenesis can help understand the role that residue plays in an interaction. It requires the synthesis of a DNA primer which contains the desired mutation and the complementary DNA template around the mutation around the mutation site. This way the primer hybridizes with the DNA in the gene.

Table 1.3 Proposed β-actin mutations.

Single Mutants	Double Mutants
V159L	V159L-S14A
V159Ile	V159L-S14V
S14A	V159Ile-S14A
S14V	V159Ile-S14V

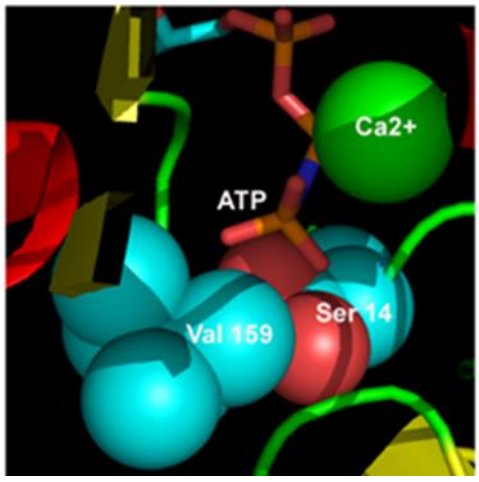

***Figure 1.12 Ribbon structure of ATP binding site**. Highlighted are the 2 amino acids of interest. Ser14 and Val159 in this 3D crystal structure (PDBID 1NWK).*

The choice of mutation to make was taken into consideration after visual inspection of 3D crystal structures of β-actin. Mutations at Ser14 and Val159 were chosen. Ser14 has direct contact with the nucleotide as it hydrogen bonds with the terminal phosphate of ATP. Val159 was chosen because it is near the binding site so a bigger, "bulkier" amino may affect the binding site, and potentially favor ADP binding over ATP binding. Single

and double mutants were made with a Quikchange II protocol.

The QuikChange II site-directed mutagenesis kit is used to make point mutations, replace amino acids, and delete or insert single or multiple adjacent amino acids. The QuikChange II site-directed mutagenesis method is performed using PfuUltra high-fidelity (HF) DNA polymerase for mutagenic primer-directed replication of both plasmid strands with the highest fidelity. The basic procedure utilizes a supercoiled double-stranded DNA vector with an insert of interest and two synthetic oligonucleotide primers, both containing the desired mutation. The oligonucleotide primers, each complementary to opposite strands of the vector, are extended during temperature cycling by PfuUltra HF DNA polymerase, without primer displacement. Extension of the oligonucleotide primers generates a mutated plasmid containing staggered nicks. Following temperature cycling, the product was treated with Dpn I. The Dpn I endonuclease is specific for methylated and hemimethylated DNA and was used to digest the parental DNA template and to select for mutation-containing synthesized DNA, as DNA isolated from almost all E. coli strains is dam methylated and therefore susceptible to Dpn I digestion. The nicked vector DNA containing the desired mutations is then transformed into XL1-Blue supercompetent cells, followed by isolation of DNA from the resulting transformants and characterization by Sanger sequencing.

1.4.6 Optogenetics

Optogenetics is a field of genetic engineering that uses light to measure, manipulate, and control biomolecular processes (41). The tools and methods developed are used to control molecular signals and understand cellular functions such as protein localization and protein-protein interactions. One primary advantage of optogenetics is that it can provide spatial and temporal control over cell signaling pathways (42).

Optogenetic tools can be divided into two groups: actuators and sensors. Opsins are actuators that are light-gated ion channels that absorb light at a specific wavelength. When activated by light the channels are opened or closed. Scientists have identified a variety of naturally occurring microbial opsins that respond to different wavelengths of light, like blue or yellow light (43). These various opsins also initiate different electrochemical responses, such as nonspecific cation influx vs. proton efflux. Researchers have used genetic engineering to improve these natural opsins by inducing point mutations to alter the absorption spectrum or adding trafficking signals to localize opsins to the cell membrane. The most common and well-known opsin is Channelrhodopsin, a foundational optogenetics tool that allows the fast depolarization of neurons upon exposure to light through direct stimulation of ion channels. Naturally occurring channelrhodopsins were discovered in the green algae *Chlamydomonas reinhardtii*. Channelrhodopsin-1 (ChR1) is excited by blue light and permits nonspecific cation influx into the cell when stimulated. Channelrhodopsin-2 (ChR2), the first widely adopted optogenetics tool, is also a blue light activated cation channel.

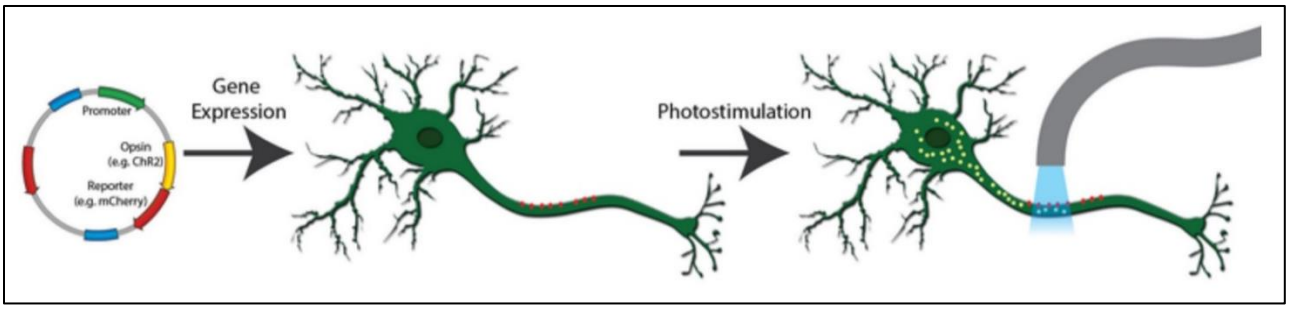

Figure 1.13. Schematic of an Optogenetics procedure *Adapted from Addgene Optogenetics. A channelrhodopsin, fused to mCherry, is expressed in neurons (red dots). When exposed to light of the correct wavelength, the pore opens, cations flow into the cell (yellow dots), and the neuron is activated.*

In this work, photoswitchable proteins will be used to control β-actin and cofilin activity. Genetically encoded photo-responsive actin and cofilin will be created by mutations. A weakly active cofilin mutant (S3E) is attached to a protein called cryptochrome 2, which is sensitive to blue light, along with mCherry which is fluorophore used as a marker (28). This will be part of a

dimer system where G-actin mutants will be attached to a fluorescent construct called Cryptochrome Interacting β-helix-loop-helix (Cib). The Cryptochrome 2-Cib system, when exposed to 488nm (blue light), will promote the interaction of the cofilin and G-actin protein.

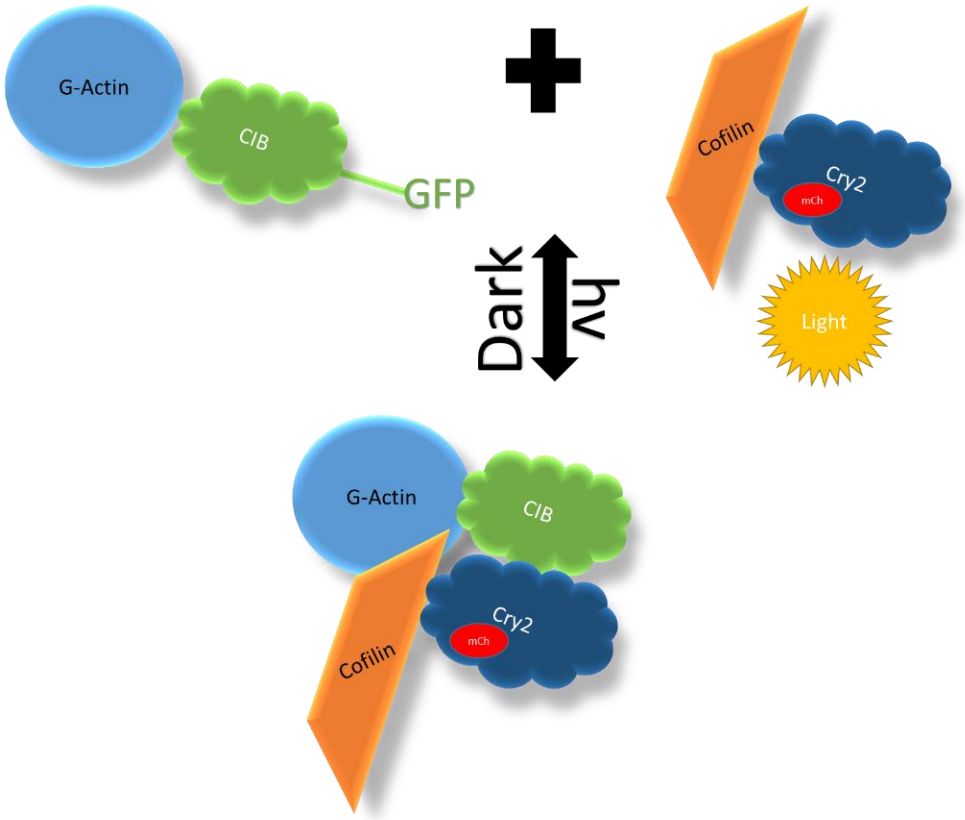

Figure 1.14 General strategy for the design of a genetically encoded light-activatable protein. *A weakly active cofilin mutant (orange) is appended to the light-responsive Cry2 (navy). In the absence of light, the cofilin construct has no discernable effect on the cytoskeleton. Upon illumination at 488 nm, Cry2 associates with Beta G-actin-bound Cib(green), furnishing a high, effective cofilin concentration, thereby promoting interaction of beta actin and cofilin.*

CHAPTER 2: Expression and In Vitro Studies

2.1 Wild-Type Protein Expression

The expression of beta-actin started with BL-21 competent cells with 1μL of the WT DNA being added, which had been confirmed by Sanger sequencing. The cells were incubated for 30 minutes on ice. The cells were then "heat-shocked" at 42 °C for thirty seconds and then put back on the ice for 2 minutes. 600μL of Super Optimal Broth (SOC medium) which is a nutrient-rich bacterial growth medium used for microbiological culture, generally of Escherichia coli was added to the cells which are then incubated (while shaking) for about an hour at 37 °C. The cells were plated on a KAN plate and incubated for 24 hours at 37 °C.

Colonies that grew were picked and inoculated overnight in 1 L of LB broth. 500 μL of isopropyl β-D-1-thiogalactopyranoside (IPTG) (500 mM stock solution) was added after the concentration of bacteria, and the optical density at 600 nm (OD_{600}) reached 0.608. IPTG is a mock lactose that triggers transcription which is the beginning of gene expression. The overnight LB broth was then divided into 200 mL bottles and centrifuged at 5000 rpm (4 °C) for 20 minutes. A pellet was formed, and the supernatant was discarded. The pellet was lysed with B-PER, which is a cell lysis reagent that is a nonionic detergent-based solution that effectively disrupts cells and solubilizes native or recombinant proteins without denaturation. Protease inhibitor was added (500 μL per 10 mL B-PER). The lysed pellet was spun down with the supernatant, and the pellet was separated and frozen at -80 °C for later use.

The supernatant was put through a Coomassie SDS-PAGE gel where we tested to see if the supernatant contained any of the beta-actin protein. Only a trace amount was detected in the supernatant (Figure 2.1), so an inclusion body preparation was done on the pellet.

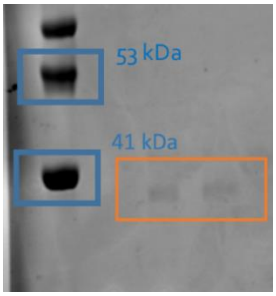

Figure 2.1 SDS-PAGE Gel of supernatant*. After the lysing of the pellet, the supernatant was analyzed using electrophoresis to see if protein had been expressed. Very little soluble protein was found in the supernatant.*

The pellet was thawed and resuspended with 10 mL of B-PER with added lysozyme (40 µL of a 10 mg/mL stock solution). A 1:10 dilution of B-PER was added to the resuspension and then sonicated. After sonication, it was centrifuged at 14000 rpm for 15 minutes. Sonication and centrifugation were repeated twice. The inclusion bodies were solubilized in 5 mL of 50 mM of HEPES with 25mM of DTT and then incubated for an hour at 4 °C and later centrifuged. The protein was diluted in 1 mg/mL in HEPES solubilization buffer.

The protein was diluted, dropwise, in refolding buffer (50 mM glycine (pH 9)/200 mM NaCl/5 mM EDTA/10 mM DTT/1X protease inhibitors) on ice and mixed. The refolding buffer was put through a spin concentrator and later dialyzed using snakeskin dialysis. The wild-type was put through a coomassie SDS-PAGE (Figure 2.2). Three very concentrated bands were formed which indicates an abundance of beta-actin protein present.

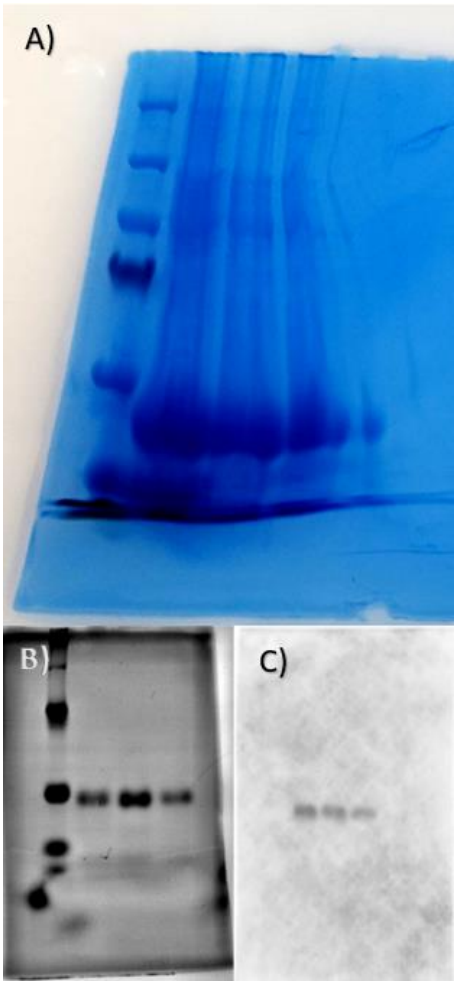

Figure 2.2 Coomassie Blue Gel of Pellet*. A) After not finding abundant protein in the supernatant, insoluble protein was identified in the cell pellet. The pellet was solubilized in GdHCl and then refolded. The solubilized protein was subjected to SDS-PAGE to find much protein. Pictured below B) the protein was refolded and C) characterized by an α-actin western blot.*

To further confirm the expression of beta-actin we used MALDI/TOF to establish the molecular weight of our protein concentrate (Figure 2.3). We detected weight of ~43 kDa, and the molecular weight of β-actin is ~42 kDa. The additional mass comes from the 6X His tag and leader sequence that results from the cloning of

our actin gene into the pNic28 expression vector. The matrix used was 10 mg/mL sinapinnic acid in 70:30 acetonitrile: water with 0.3% trifluoroacetic acid. Sinapinnic acid is very a common matrix used for large peptides and proteins and has the ability to absorb laser radiation and donate protons to the analyte of interest which is the beta-actin protein.

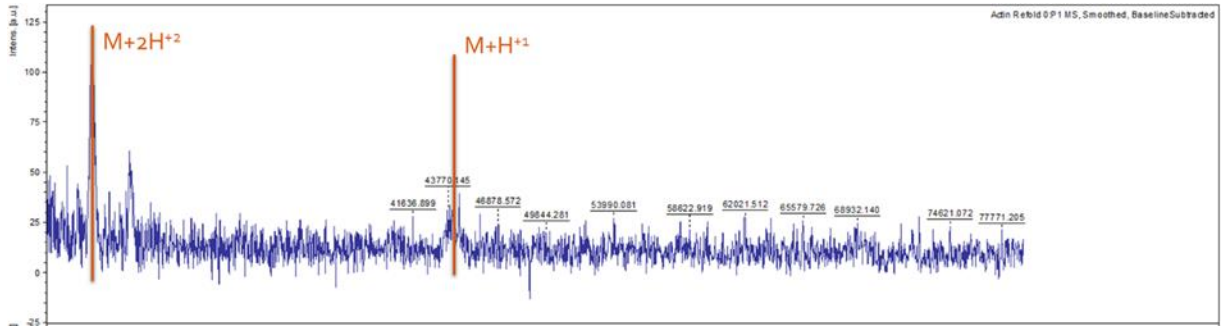

Figure 2.3 Beta-Actin MALDI/TOF*. The peak labeled M+H is the analyte when a protein is absorbed and is the indicator of the analyte and its molecule weight. The weight is 43710 da. The literature weight of Beta-actin is about 42 kDa. The additional mass (1700 da) corresponds to the presence of a N-terminal 6X His affinity tag and the associated leader sequence.*

2.2 Circular Dichroism

Using circular dichroism, we tried to monitor if there are any changes in the structure of actin when bound to different nucleotides. For these studies, we initially used purified WT actin from the soluble fraction of our bacterial lysate. These initial studies produce noisy CD spectra whose overall shapes did not match literature spectra of over-expressed β-actin (Figure 2.4). We followed up these efforts by performing CD of refolded actin, prepared via the following protocol: 500 µL of the wild-type protein (3.215 mg/mL isolated from an inclusion body prep) was added dropwise into 40 mL of refolding buffer with dithiothreitol (pH 9). A gravity column was made with Ni-NTA resin which used in expression and purification of the protein. The resin purifies high levels His-tagged fused proteins that are used during expression. The nickel column was first washed with wash buffer (20 mM PBS/imidazole). All 40 mL of the refolding buffer now containing the WT protein was put through the column. 10 mL of wash buffer was placed into the column, and then 7 mL of elution buffer was put through to elute the protein off the column. The imidazole is used to elute all proteins that contain the His tags. The eluted protein was then spun

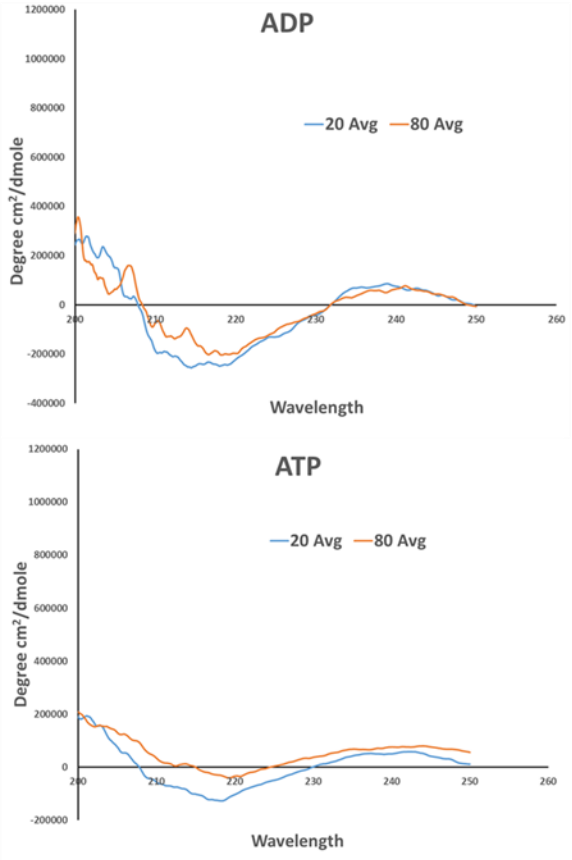

Figure 2.4 CD spectra of ATP-actin and ADP-actin *Actin CD spectra were of insufficient quality. Alternate approaches to sample prep failed to improve the observed CD spectra. A CD spectrum (bottom panel, inset) of native (solid line) and heat denatured (dashed line) ATP-actin from Eur. J. Biochem. 267, 476-486 (2000) is shown for comparison.*

down using a spin concentrator at 4000 rpm for about 40 minutes the eluted protein was spun. About 9 mL of protein was left, and the concentration was found via spectroscopic assay to be 0.9 mg/mL.

The eluted protein was put through a ZEBA column to get rid of the imidazole. The column was prepared first by washing the column with G-buffer containing ATP to do our buffer exchange and have out expressed protein bind to ATP. The column washed and spun 3 times with G-buffer and one time with our eluted protein. CD was run and unsuccessful.

Next, we attempted the refolding of actin in the presence of 2 mM Mg^{2+} and Ca^{2+} in the refolding buffer. Mg and Ca bind to actin and are important for structural integrity. The refolding buffer containing Mg^{2+}/Ca^{2+} and our refolded WT actin protein was put through the nickel gravity column. Instead of desalting using a ZEBA column, snakeskin dialysis was performed in a 1:10 dilution of G-Buffer. The CD spectra indicated that traces of imidazole were present in the protein prep. The solution was re-dialyzed and the CD

analysis repeated with no success (i.e., no spectra were observed in these studies, indicating a possible loss of protein during dialysis).

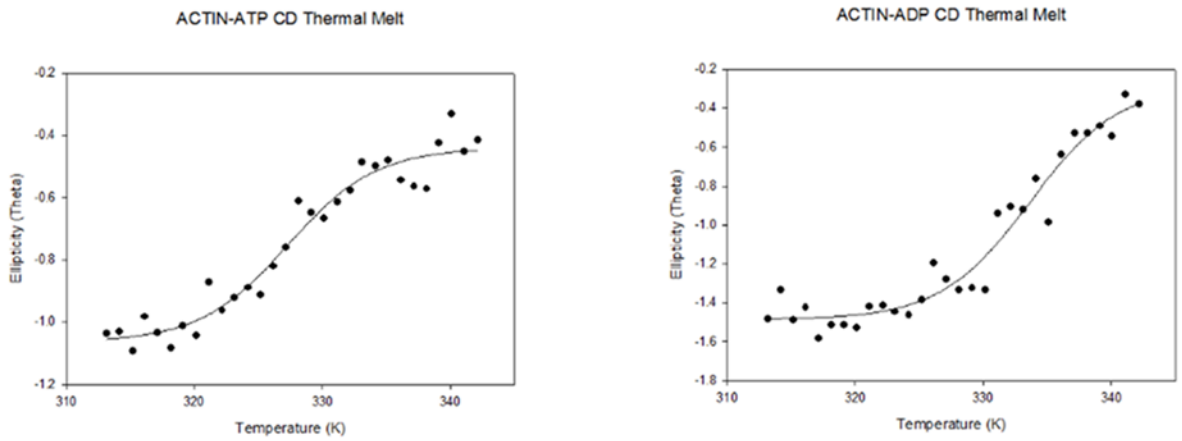

Figure 2.5 CD Thermal Melt *Curve for Actin-ATP where the Tm value is 327.3 K (.98) Actin-ADP tm value is 333.6 K (.71). The literature Tm value (variously reported from 58 – 61 ℃) for ATP-actin did not match our results (54.15 ℃).*

2.3 Thermal Shift Assay

These assays quantify the change in thermal denaturation temperature of protein in the presence of a stabilizing ligand. There are many forms of this assay, and the cellular thermal shift assay was performed. This method monitors the binding of protein by precipitation which is initiated when a protein is denatured.

The soluble fractions of the thermally denatured proteins are analyzed by a western blot, which enables detection of a melting curve. First, we tested the binding affinity of our expressed protein to ATP. The expressed protein, along with ATP, was put through a heat gradient (55-65 C) (Table 2.1). The sample was then centrifuged to separate soluble from insoluble protein, and the soluble protein was characterized by an α-actin western blot.

In our assay, 15 µL of dialyzed protein and G buffer (ddH2O, 2 mM Tris-Cl, 2 mM CaCl2) were mixed in 12 individual samples. These samples were divided in half where six samples had 4 µL of ATP added and six without ATP. The samples were heated in a PCR thermal cycler (55

Table 2.1 Temperature Gradient for Thermo-Cycler

Column Number	Temperature °C
1	55.0
2	55.2
3	55.8
4	56.7
5	57.8
6	59.1
7	60.4
8	61.7
9	62.9
10	63.9
11	64.6
12	64.9

°C-65 °C) and cooled for 3 min at room temperature. Protein was transferred to 1.5 mL tubes and centrifuged at 17000 rpm for 20 minutes. Loading dye for a western blot was added. Transfer western blot was performed for 70 mins at 140 volts. The transfer membrane was placed in 1: 500 β-actin primary antibodies overnight in a rocker. The membrane was washed with TBST, and then anti-mouse secondary was added to 5% BSA-TBST, and then the secondary was added to the membrane. The membrane was put in the imager. This assay was unsuccessful. While we were able to observe our positive control band on the western blot, no bands were observed in the actin samples that were subjected to thermal denaturation. Once heated in the thermal cycler we did not see any bands on the western blot, indicating loss of all protein during the denaturation step. As a result, we then moved on to another method of testing the nucleotide binding of our expressed wild-type protein.

2.4 Nucleotide Binding Assays

We next attempted to monitor nucleotide binding of our expressed protein, both wildtype and mutants, after the thermal shift assay. We utilized a fluorescent analog of ATP to monitor the binding of ATP and ADP to our expressed protein. Numerous analogs have been synthesized and used to probe and study ATP. They are used in many ways including the detection of ATP binding sites (Figure 2.6).

They are many types of analogs, and they can be modified in three different ways on the phosphate tail, the 2, 3 ribose group, or the base of the ATP. The experiment will determine the type of analog that is used. For this experiment we are testing nucleotide binding to a beta-actin

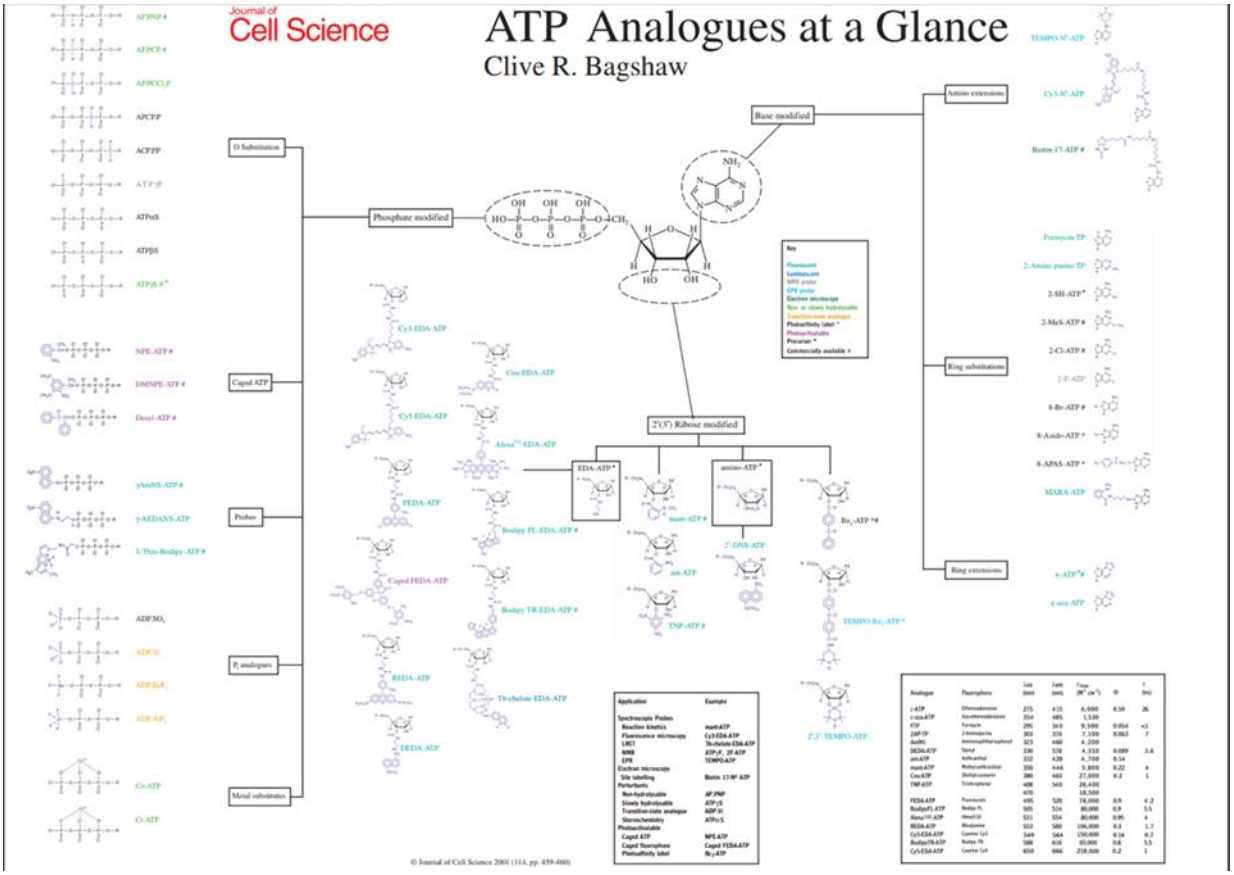

Figure 2.6 ATP Analogues. *Listed are the different types of ATP analogs. ATP analogues can be modified at the phosphate group, the base, and the ribose. Clive R. Bagshaw, J. Cell Science (2001), 114, 459-460.*

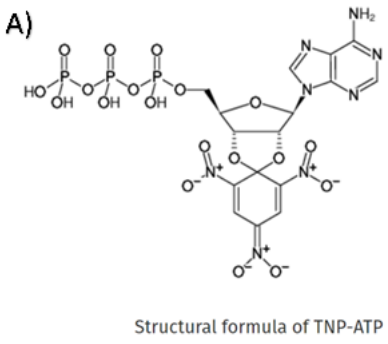

Figure 2.7 Analogs used in an assay*. A) TNP-ATP and B) Etheno-ATP.*

binding site, so a phosphate tagged analog would not work. The 2 analogs chosen were TNP-ATP and etheno-ATP (ε-ATP), modified at the ribose and base position respectfully (Figure 2.7).

We performed an ATP exchange assay to monitor the exchange of regular ATP and the fluorescent ATP. An ATP-G buffer mixture was made which contains 1 mL of 10X G-buffer, 9 mL of double-distilled water (ddH_2O), and 3 mM of ATP and ADP. The expressed protein was spun with the ATP-G buffer mix in a spin concentrator. The spun protein is

plated, and the fluorescent ATP is added and immediately put into the reader. The results were not conclusive and consistent results were not able to be collected. The spectra displayed a change of fluorescence which indicated some nucleotide binding, but concrete results were not obtained from this study.

2.5 Mutagenesis

Our site-directed mutagenesis started with a template made from the wild-type actin DNA. A DNA plasmid kit (EZ DNA Plasmid MIDI Kit) was used to extract DNA that would later be used as the template for the mutations. The method of plasmid preparation and extractions begins with the growth of the culture. The Actin PNIC28 was added and grown in 30 mL of kanamycin-LB media overnight. A pellet was created by centrifugation at 4000Xg for 10 mins. The pellet was resuspended in RNase A then lysed using Omega's Lysis buffer. The pellet was then neutralized by a neutralization buffer and centrifugation. The supernatant is added to a 'HiBand' DNA column where the DNA binds to a membrane on the column. The column is then washed 3 times with wash buffer, and the DNA is eluted out. The concentration was checked afterward, and it was about 200 mg/mL

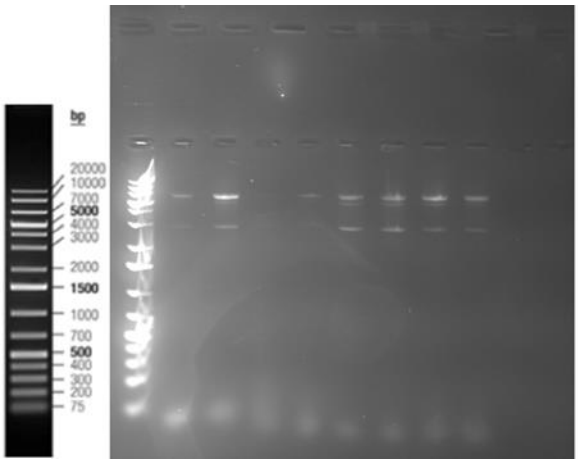

Figure 2.8 Agarose Gel for S14A/S14V primers. *Lane 1: 1 kB DNA ladder. Lanes 2-5:mutagenic PCR reactions generated with S14A mutagenic primers; lanes 6-9: mutagenic PCR reactions using the S14V primers. The PCR reactions from the 2nd S14A lane and the 2nd and 3rd S14V lanes were transformed into ultracompetent E. coli and transformants characterized by Sanger sequencing.*

To perform the site-directed mutagenesis, we added site-directed reverse and forward primers (IDT DNA, Inc.). The template and primers were mixed with nuclease-free water and a reaction mix from a commercial DNA polymerase kit.

Thermal cycling was performed using an Eppendorf PCR thermocycler. Agarose Electrophoresis was performed to confirm DNA amplification.

The DNA that showed the greatest amplification were chosen for DPNI digest and transformation in ultra-competent cells (Figure 2.8). Shown in Figure 2.8 are the results of site-directed mutagenesis PCR for the S14A and S14V primers. Transformation of the S14A primers did not produce any colonies. The S14V produced colonies which were picked and put into 10 mL of terrific broth. A plasmid preparation protocol (mid-prep) was performed, and the resulting DNA was sequenced. The mutants that came back that correct and ready for experimentation were the single mutants Val159Leu, Val159Ile, Ser14Val and double mutants Val159Leu-Ser14Ala, and Val159Leu-Ser14Val.

CHAPTER 3: OPTOGENETICS

3.1 Theory

Optogenetics is a field of genetic engineering that uses light to measure, manipulate, and control biomolecular processes. Optogenetic tools can be used to control cell signaling. The primary focus of this work is to create optogenetic constructs for the control and monitoring of cofilin-actin rod formation. Ultimately, we aim to study cofilin-actin rods and their role in the pathology of AD in neural cells.

Cofilin-actin rod formation, which was discussed in chapter 1, is associated with AD and causes synaptic dysfunction of neurons. Multiple factors contribute to the formation of cofilin-actin rods: elevated levels of active cofilin, elevated levels of ADP-actin, and a highly oxidative environment. The assay we perform has to simulate these conditions. We can recreate these conditions by inhibiting mitochondrial function by using an azide solution. Azides uncouple oxidative phosphorylation and inhibit ATPase activity but not the ADP-ATP exchange reaction (44). We can recreate high ADP concentration by putting the cell under energetic stress by inhibiting glycolysis. D-deoxyglucose (2-Deoxy-D-glucose) is a glucose molecule which has the 2-hydroxyl group replaced by hydrogen so that it cannot undergo further glycolysis. As such, it acts as a competitive inhibitor of the production of glucose-6-phosphate from glucose.

A flavoprotein called cryptochrome 2 (Cry2) will be used to control our optogenetic constructs in tandem with a beta helix loop helix (bHLH) protein called CIB. Cry2, a blue light photoreceptor protein from *A. thaliana*, and CIB comprise a light responsive protein dimerization module. Cry2 has a chromophore called flavin which absorbs at a wavelength of 450 nm. The Cry2/CIB binds together to form a dimer in blue light and dissociates in the dark. For our optical switch, we will utilize the proteins Cry2 infusion with mCherry (a fluorescent marker) and cofilin

(Cry2-mCh-Cof) and CIB infusion with actin and the fluorescent marker GFP (Actin-CIB-GFP). In addition to WT β-actin, we have created β-actin mutations that will also be used in our optogenetic construct single mutants Val159Leu, Val159Ile, Ser14Val and double mutants Val159Leu-Ser14Ala, and Val159Leu-Ser14Val.

3.2 Prior Studies and Results:

Previous Studies of cofilin-actin rods have been performed but have been hampered by various experimental challenges (45). For example, cofilin-actin rods have been successfully induced in cells in the presence of azide, but they require antibodies for detection via immunostaining, which prevents real-time assays of rod formation.

In another study mutant cofilin, Cofilin R21Q was linked to a red fluorescent protein (mRFP) to monitor cofilin-actin rod formation. The CofR21Q-mRFP showed oxidant-inducible rod formation, but it was irreversible without a change in cell media. The construct we plan to will be reversible, enabling greater experimental control (46).

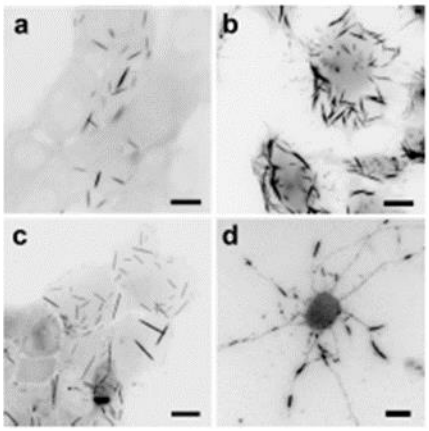

Figure 3.1 Example induces rod formation in cultured cells*. All panels are inverted fluorescence images. A) is GFP rods in A4.8 cells. B), C), D) are cofilin rods in Hela cells, A431 cells, and rat cortical neurons respectively. Image reproduced from J Biol Chem. 2010 Feb 19;285(8):5450-60.*

Previous studies have used the Cry2/CIB construct to control protein's activities with light activation. This includes proteins like Cre recombinase which is an enzyme derived from P1 bacteriophage. It plays a role in site-specific recombination events and its used to manipulate DNA in both in vivo and in vitro lab work (47). BAX, which is part of the Bcl-2-gene family which is have been used the Cry2/CIB construct to

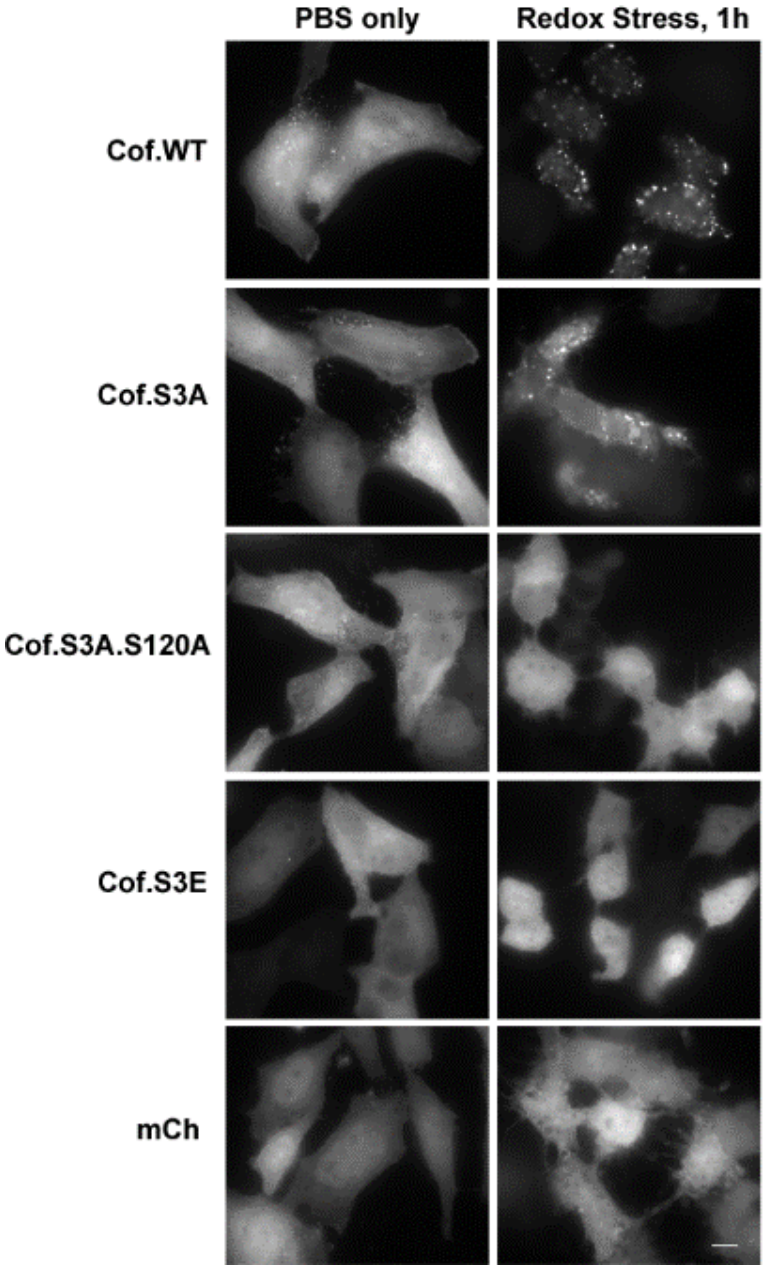

Figure 3.2 Responses of cofilin mutants to oxidative stress. *Cofilin (WT, S3A, and actin-binding impaired mutants) exposed to oxidative and energetic stress in transiently transfected HeLa cells. After 1 hour in 6mM D-deoxyglucose and 10 mM sodium azide, significant cofilin-actin clustering is detected in the WT and S3A cofilins, but not in the actin binding impaired cofilins or the mCherry control. Scale bar = 10 microns.*

initiate cell death (48). Our laboratory has created many cofilin mutants and fused them to Cry2, where Cry2 was either bound at the C- or N-terminus (Table 3.1).

The Cry2/CIB interaction has also been used in protein translocation. Cry2/CIB has been used to move cytosolic proteins to other locations within a cell such as the plasma membrane and mitochondrial outer membrane in response to light (Figure 3.3).

We have generated constructs that fuse Cry2 with various mutants of cofilin and Cib with beta-actin. In our initial work, we demonstrated a wild-type cofilin fusion fused to Cry2 (Cof. WT-Cry2-mCh) forms constitutive, light-independent clusters/rods under oxidative and energetic stress (Figure 3.2). This result indicates that, when

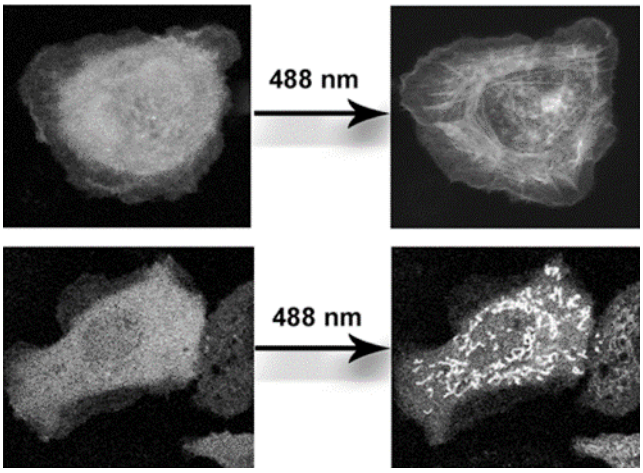

Figure 3.3 Examples of light activated translocation. *Blue light (488 nm) stimulation of transfected cells induces recruitment of Cry2.mCherry to F-actin (top; co-transfected with LifeAct-CIB) or the outer mitochondrial membrane (bottom; co-transfected with Tom20-CIB).*

placed under oxidative stress, our Cry2-Cof fusions can interact with endogenous actins in a manner similar to endogenous cofilin.

Various N- and C-terminal cofilin/Cry2 mutant fusions were constructed with beta-actin/CIB(Table 3.1). Cells were transfected with these various constructs and were put under oxidative stress and energetic stress. The Cry2-Cofilin fusion Cry2-mCh-Cof.S3E, in combination with beta-actin-CIB (Table 3.1, Row VII), demonstrated the rapid & reversible formation of cofilin-actin clusters in response to 488 nm light stimulation under cofilin-actin rod forming conditions. Control experiments (conducted with optogenetic actin alone and optogenetic cofilin alone) demonstrated that both cofilin and actin are required for light-induced rod formation. Cof.S3E, which mimics the phosphorylated state of cofilin at Serine 3, does not

Table 3.1 Summary of cofilin constructs. Survey of light-stimulated cofilin-actin rod formation of various N- and C-terminal cofilin mutant fusions to Cry2 in the presence of 10 mM Azide/6 mM D-deoxyglucose.

	N-terminal Cofilins	Effect of Light Stimulation
I	Cof.WT-Cry2/bActin-Cib	Constitutive clusters; irreversible
II	Cof.S3A.S120A-Cry2/bActin-Cib	**Abundant Reversible Clusters *(5/6)***
III	Cof.S3E-Cry2/bActin-Cib	Some cells form light induced clusters (4/8)
IV	Cof.S3A.S120A-Cry2/**Cib-ONLY**	No clusters
	C-terminal Cofilins	
V	Cry2-Cof.WT/bActin-Cib	Constitutive clusters; irreversible
VI	Cry2-Cof.S3A.S120A/bActin-Cib	Constitutive clusters; irreversible
VII	Cry2-Cof.S3E/bActin-Cib	**Abundant Reversible Clusters (8/8)**
	No Cofilin Controls	
VIII	Cry2-mCh/bActin-Cib	Some cells form light induced clusters (3/10)
IX	Cry2-mCh/**Cib-ONLY**	No clusters

bind or sever F-actin, and furthermore, cannot be dephosphorylated by SSH-1, which is the primary driver of cofilin activation under oxidative/energetic stress. This makes it an ideal cofilin mutant for inclusion in an optogenetic switch, since it is mostly bio-orthogonal, and, in contrast to Cof.WT will only incorporate into cofilin-actin rods in cells under oxidative/energetic stress when triggered with light.

3.3 Experimental Design:

The purpose of our experiment is to investigate whether the proposed mutations to β-actin favor the ATP-bound form or the ADP-bound form. We are using its interaction with cofilin under oxidative stress as a reporter of the nucleotide-bound state of β-actin. We monitor the nucleotide binding state of the β-actin under two conditions: cells with oxidant and cells without an oxidant. If rods and clusters form without our oxidant (10 mM Azide/6 mM D-deoxyglucose), actin is presumed to be primarily in the ADP-bound form of actin. If rods form with our oxidant only, then β-actin is presumed to be primarily in the ATP-bound form.

To test our mutant constructs, we transfected them into a HeLa cell line, an immortal human cancer cell line. **Cell passaging**: The cells were first aspirated to remove the media present. The cells were washed with 5 mL of PBS. The PBS was then aspirated and discarded. About 5 mL of trypsin was used to wash away cells from the walls of the dish. Trypsin is a cell protease that breaks down all the proteins on the surface of a cell. The dishes were then put into an incubator for 10 mins at 37 °C. The dishes are removed from the incubator and 10 mL of cell media (DMEM). The media was pipetted up and down to spread the cells evenly around the dish. The cells were counted using a hemacytometer. After the cells are counted, they were incubated for 48 hours and then ready for transfection.

3.3.1 Assembly of Optogenetic Constructs

Cofilin and Cry2PHR were amplified separately by PCR with Phusion polymerase. After gel isolation of the PCR fragments, aliquots of the purified DNA fragments were combined [6 µL of each PCR fragment, 1.5 µL of F and R primer (20 µM stocks), 4 µL dNTPs (2.5 mM stock), 3 µL of 10X Phusion HF buffer, 8 µL ddH2O, and 0.5 µL Phusion] and subjected to overlap extension PCR. The resulting appropriately sized PCR fragments were gel isolated, purified, and subjected to restriction digest. The resulting fragments were then ligated into mCherry-N1 with βsRGI and NotI sites to give Cry2-mCh-Cof.S3E.

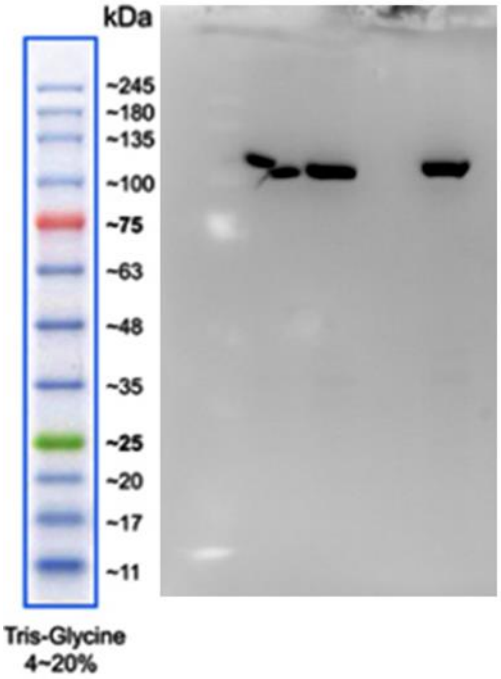

Figure 3.4 Western Blot of β-actin-CIB-GFP. *α-GFP western blot of transfected HeLa cell lysates reveals bands corresponding to: actin.S14V (lane 1); actinV159I (lane 2); actin S14V.V159L (lane 3).*

Our expressed WT and mutant beta-actin were fused with CIB to create a β-actin-CIB-GFP construct. CIBN and β-actin (WT and mutants) were amplified separately by PCR with Phusion polymerase. After gel isolation of the fragments, aliquots of the purified DNA fragments were combined (6 µL of each PCR fragment, 1.5 µL of F and R primer (20 µM stocks), 4 µL dNTPs (2.5 mM stock), 3 µL of 10X Phusion HF buffer, 8 µL ddH2O, and 0.5 µL Phusion) and subjected to overlap extension PCR. The resulting construct was subjected to restriction digest with XhoI and HindIII enzymes and then ligated into analogously digested phCMV-GFP vector (Genlantis).

Both the cofilin and β-actin were transfected into the Hela cells. A lipid-based transfection technique was used. We will create a 1:1 transfection solution. Solution 1 contains 1250 ng/µL of DNA of the protein of interest. 5 µL of P3000™ Reagent, which is an enhancer, is added along

with 125 μL of the Opti-MEM I medium. Solution 2 contains 125 μL of the Opti-MEM medium and 3.73 μL of Lipofectamine which increase the transfection efficiency of RNA or plasmid DNA into in vitro cell cultures by lipofection. Lipofectamine reagent contains lipid subunits that can form liposomes in an aqueous environment, which entrap the transfection payload (49). Both are mixed and added to the Hela cells. The cells are then wrapped in foil to hide them from light and incubated for 24 hours.

The Leica DMi8 Live Cell imaging system was used to image the cells. The infinity scanner allows us to manipulate the light source and record the cell activity during the experiment. Before imaging, we added our control PBS, which was a part of the media and to maintain normal pH. We took images over 10 mins with 470 nm of light and then after light exposure, capture 10 mins worth of images in the absence of 470 nm light. We later added the 10 mM Azide/6 mM D-deoxyglucose oxidant to induce cell stress and rod formation.

3.4 Results

Of the mutants that had been transfected, Val159Ile, Ser14Val, and double mutant Val159Leu-Ser14Val, the Ser14Val and Val159Leu-Ser14Val formed rods. Light-induced clusters of cofilin-actin were present in all three mutants (Table 3.2).

The S14V single mutant had multiple rods form in all samples taken, with the average of 2 rods per cell (±1) and an average length of 7.42 μm (±.68). Cofilin-actin rods had formed before our 10 mM Azide/6 mM D-deoxyglucose oxidant was added (Figure 3.5). Rods had already formed before the addition of the oxidant providing evidence that the ATP binding site has been changed and that ADP binding is favored (Figure 3.7). We monitored the fluorescence of the rods during light exposure and when the light is off. After light exposure, the fluorescence does increase

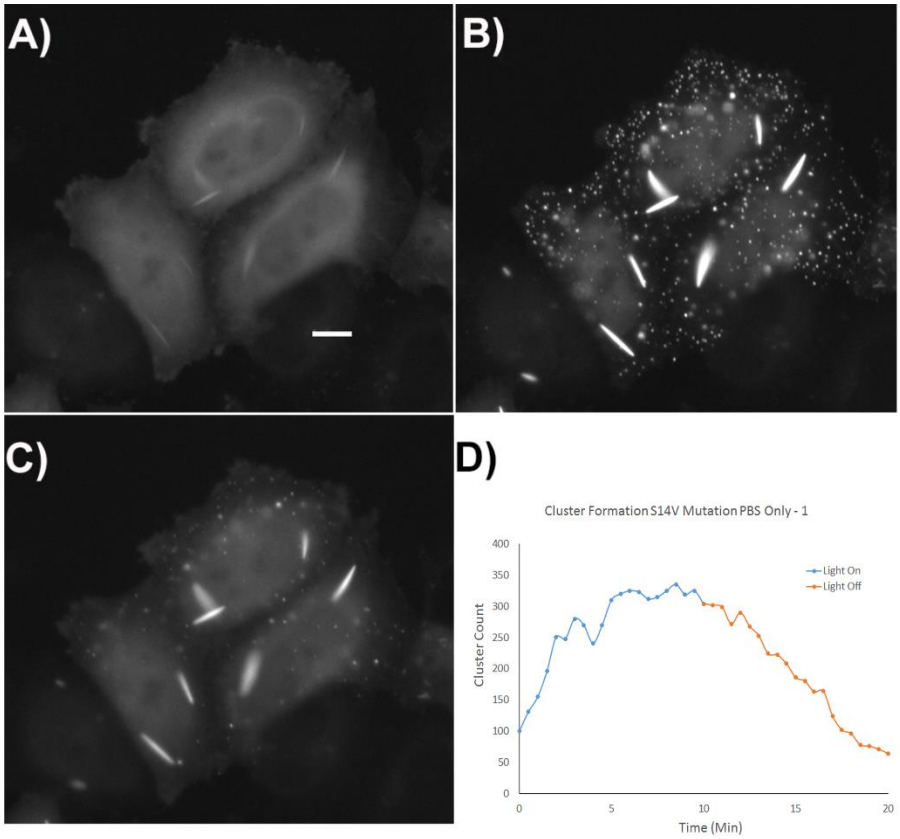

Figure 3.5 S14V mutant. Sample 1 *A) The region of cells before Light exposure B) Cells after 10 mins of light exposure C) Cells after 10 mins of cell in the dark after initial exposure D) Graph of the amount of cluster formed and dissipated over time. Scale bar = 10 microns.*

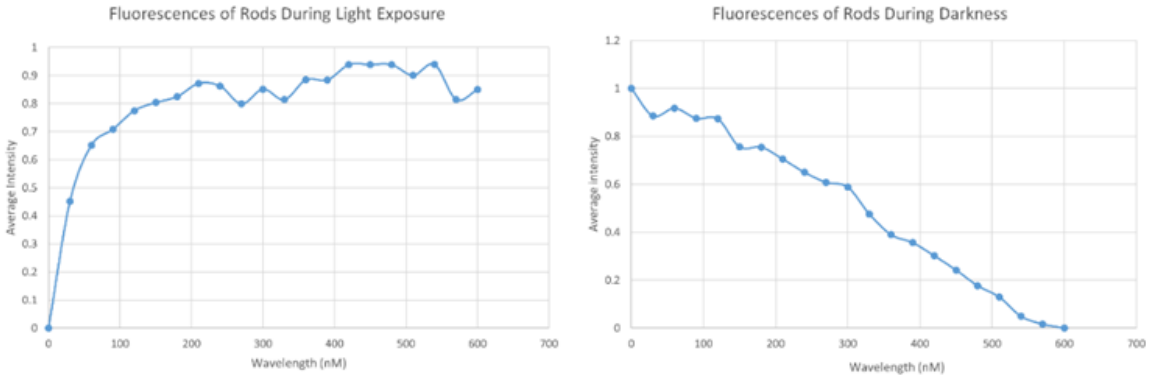

Figure 3.6 Z-Plot of S14V Rods. *The fluorescence of the rods are measured and when the cell is stimulated by light the rods overall fluorescence increases and when the cell is in darkness the fluorescence decreases. This also correlates with rod size and cluster count.*

as the rods aggregate more of the Cry2.mCh.CofS3E but starts to plateau. When the light is not emitted the fluorescence decreases over time while the rods visibly shrinks in size (Figure 3.6).

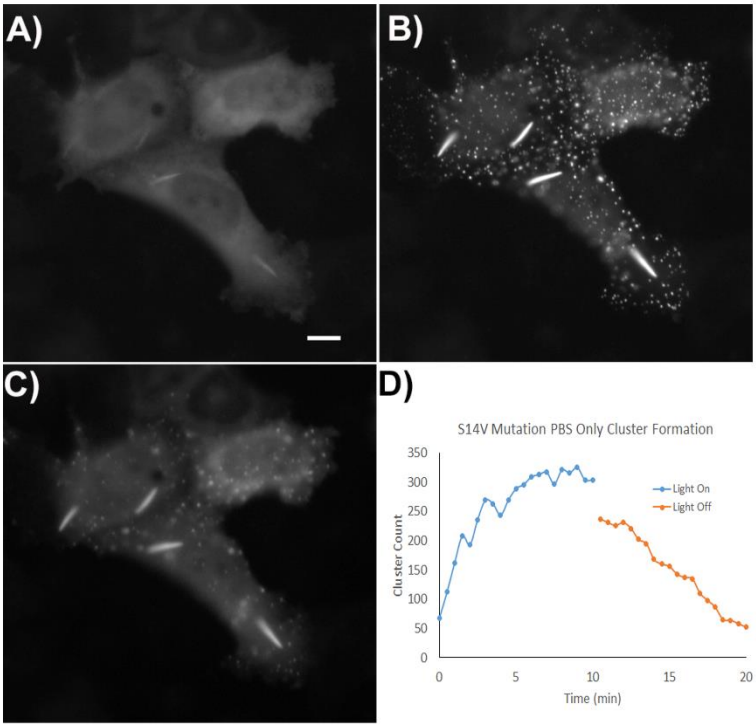

Figure 3.7 S14V mutant. Sample 2 *A) The region of cells before Light exposure B) Cells after 10 mins of light exposure C) Cells after 10 mins of cell in the dark after initial exposure D) Graph of the amount of cluster formed and dissipated over time. Scale bar = 10 microns.*

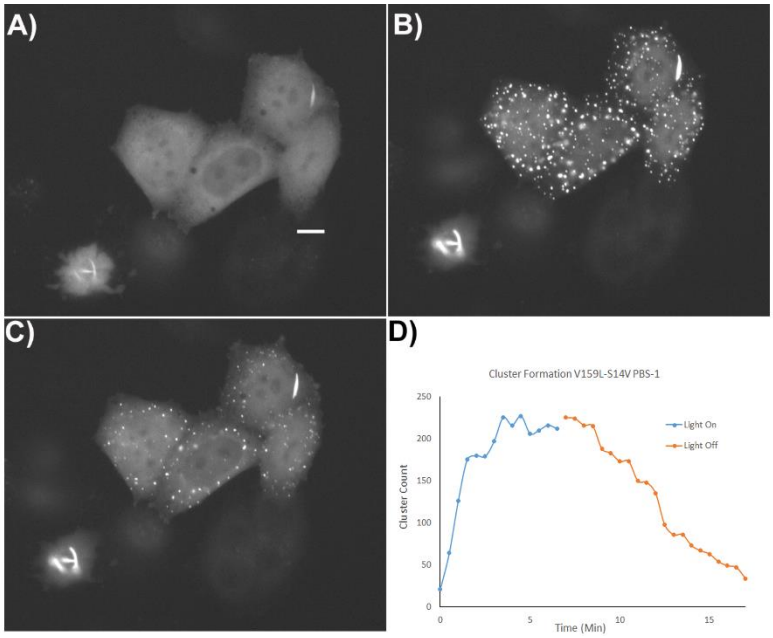

Figure 3.8 V159L-S14V double mutant. Sample 1 *A) The region of cells before Light exposure B) Cells after 7 mins of light exposure C) Cells after 10 mins of cell in the dark after initial exposure D) Graph of the amount of cluster formed and dissipated over time. Scale bar = 10 microns.*

The V159L-S14V has well-defined rods and clusters (Figure 3.8 and 3.9). There is an

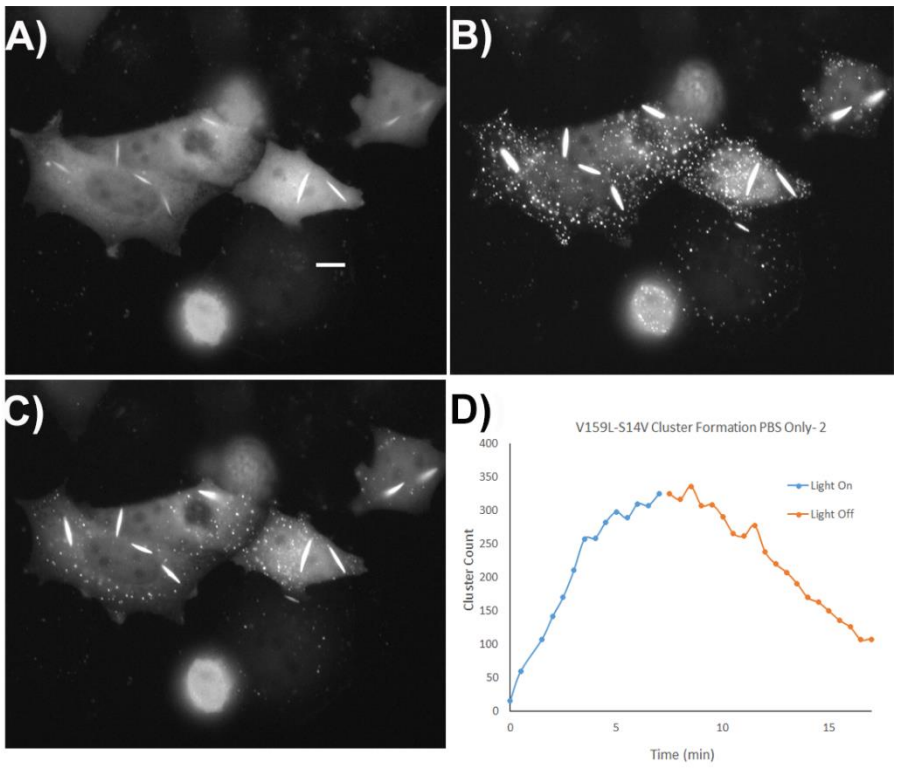

Figure 3.9 V159I-S14V double mutant. Sample 2 *A) The region of cells before Light exposure B) Cells after 7 mins of light exposure C) Cells after 10 mins of cell in the dark after initial exposure D) Graph of the amount of cluster formed and dissipated over time.*

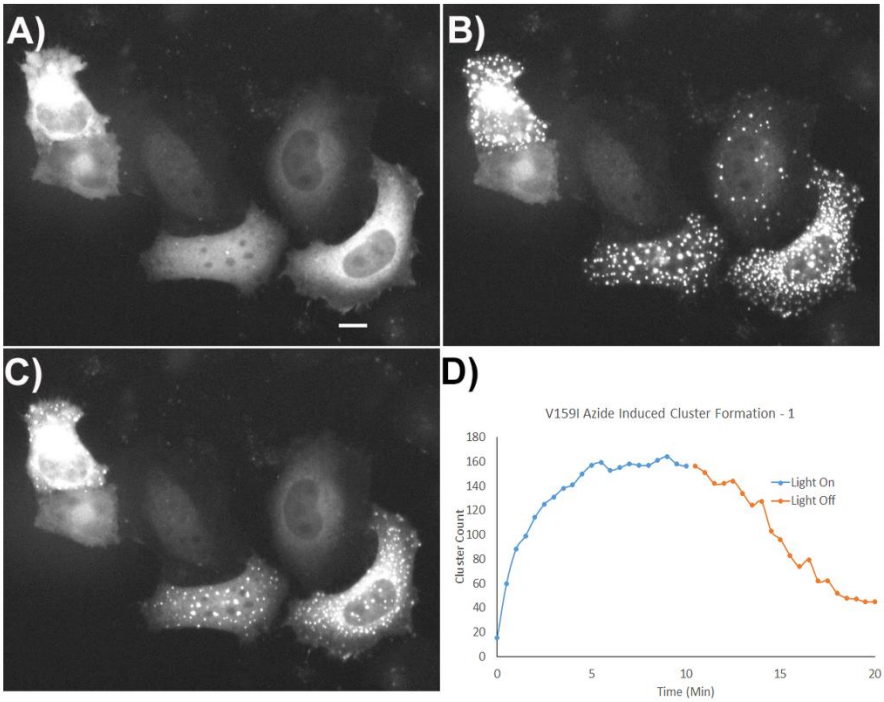

Figure 3.10 V159I Mutant. Sample 1. *The cell was induced with a 10nM sodium azide solution A) The region of cells before Light exposure B) Cells after 10 mins of light exposure C) Cells after 10 mins of cell in the dark after initial exposure D) Graph of the amount of cluster formed and dissipated over time*

average of 4 rods per cell (+2) with an average length of 6.22 μm (±.43). Rods were also present

Table 3.2 Summary of Actin

Construct	PBS Only	PBS With Azide
Wild Type	No Rods or Clusters	Ample Amount of Clusters
S14V	Abundant Rods and Clusters	Some Rods and Clusters
V159L-S14V	Abundant Rods and Clusters	Abundant Rods and Clusters
V159I	No Rods or Clusters	Ample Amount of Clusters

Survey of the 2 conditions and the 3 transfected construct in HeLa Cells. The S14V mutations created rods without the stimulated oxidative stress. In the presence of oxidant, the V159I mutant did have clusters displaying nuclear localization.

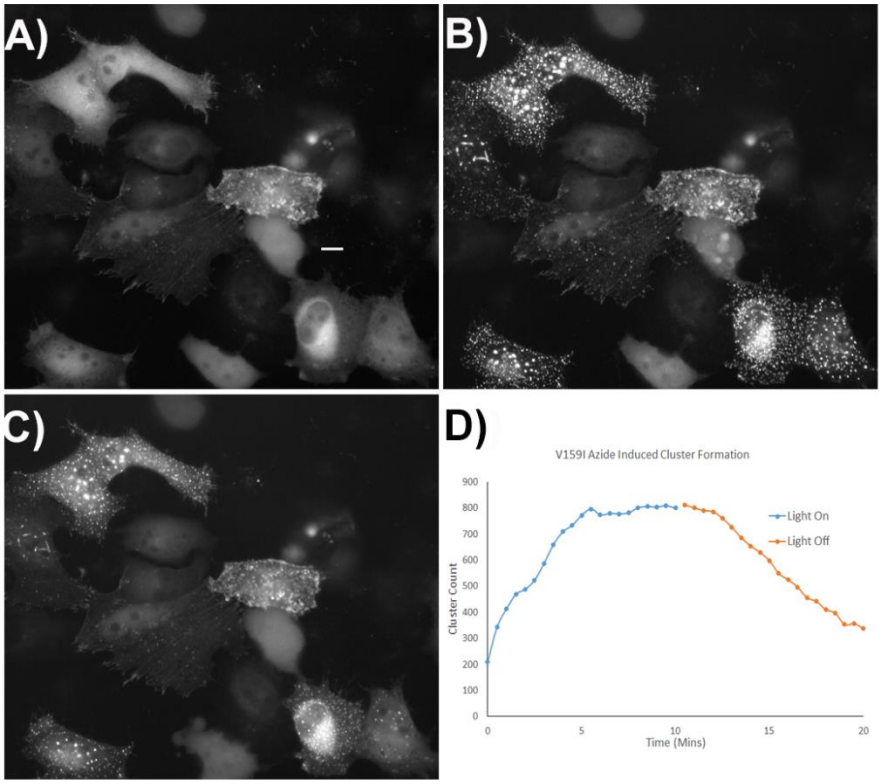

Figure 3.11 V159I Mutant. Sample 2. *The cell was induced with a 10nM sodium azide solution A) The region of cells before Light exposure B) Cells after 10 mins of light exposure C) Cells after 10 mins of cell in the dark after initial exposure D) Graph of the amount of cluster formed and dissipated over time*

before adding any oxidant meaning that ADP-actin binding is favored. As we observe the time lapse of the cell imaging, the number of clusters, the size or rods, and the fluorescence are all reversible and rapidly dissociate in the dark.

The other successful transfection was the Val159Ile mutant. When the cells were exposed to just PBS, the cells did not create rods, but rapid and reversible clusters were formed. So, we exposed the cell with our azide solution to see if the mutation would still form rods. More clusters were formed but lacked rods (Figure 3.10 and 3.11)

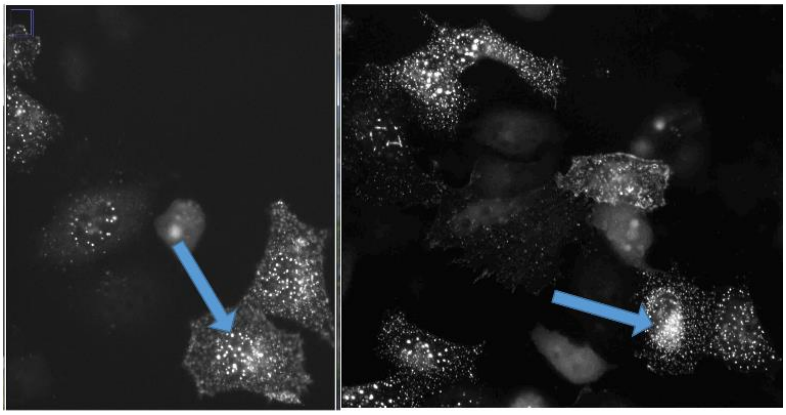

Figure 3.12 V159I displaying nuclear localization. *The cofilin-actin cluster that formed in the V159L exhibited light-inducible nuclear localization, which could be used in a separate study probing the role of actin in gene transcription.*

The V159I mutant formed clusters in and around the nucleus of the cells displaying nuclear localization (Figure 3.12). Recent research has shown that actin plays a role in gene transcription and binds to specific transcription factors (50). This can be used as a tool to study actin dependent transcription. This study showed that the single amino acid change for serine to valine displaced a shift in affinity to ADP-actin. The change to an amino acid that does not make hydrogen bonds to the terminal phosphate of ATP, likely rendering actin in its ADP-bound state. Both the S14V and the V156L-S14V double mutants showed behavior associated with the ADP-bound form of actin.

CHAPTER 4: CONCLUSION

4.1 Summary

The work detailed in this thesis document has shown the process of developing a protocol for overexpression in E. coli. Due to our low quantity yields of active β-actin protein from the IMAC purification method, the inclusion body prep method was used. The method produced a higher yield of active β-actin and then allowed us to perform several assays to assess actin.

A variety of assays were used to test nucleotide binding of our expressed actin. Circular Dichroism was used to identify if there was any structural change in the expressed actin when bound to a nucleotide. Our experiment was based on a literature protocol, and unfortunately, these initial studies produced noisy CD spectra's whose overall shape didn't match the literature spectra for β-actin. We followed up by performing CD on our refolded expressed β-actin. Once again, no spectra were observed in these studies indicated a loss of protein during dialysis of the refolding process.

The thermal shift assay was to quantify the change in thermal denaturation temperature of our expressed β-actin in the presence of a ligand. The method we choose as the cellular thermal shift which monitors the binding of protein by precipitation which is activated when a protein is denatured. While we were able to observe our positive control band on the western blot, no bands were found in the actin samples that were subjected to thermal denaturation. The next step is to see if the expressed protein could bind to the nucleotide. Analog ATP was used to monitor ATP binding and using different literature sources and protocols, etheno-ATP and TNP-ATP used to find binding. A spectrofluorimeter was used to detect the fluorescents of the displaced

ATP with the analog ATP. The results were not conclusive and consistent results were not able to be collected. The spectra displayed a change of fluorescence which indicated some nucleotide binding, but concrete results were not obtained from this study.

Our assays with overexpressed β-actin were mostly unsuccessful, as we experienced problems with reproducibility. Some of these problems may be due to the challenges of expressing large quantities of actin in its active form. Where true success was found was our mutagenesis and the optogenetic constructs of cofilin and beta-actin. Hela cells were transfected with β-Actin – CIB- GFP (β-actin.CIB.GFP) mutants and Cry2-mCherry–CofilinS3E (Cry2.mCh.CofS3E), then cells were treated with different treatment solutions of Sodium Azide and DeoxyGlucose in PBS. Images were taken for cells before, during and post of blue light exposure.

We successfully found three mutants of beta-actin that can produce cofilin-actin rods and clusters when stimulated by light. The mutations S14V both single and double demonstrate a change in affinity to ADP while the V159I mutant shows signs of nuclear localization which can lead to future studies into the actin-dependent transcriptions.

The discussion is that cofilin-actin rods only form under oxidative stress. β-actin nucleotide affinity is usually towards ATP where stress is needed to dephosphorylate ATP to ADP to form rods. The S14V and S14V-V159L double mutant both didn't require an oxidant ((PBS only) conditions to form clusters mean that we changed the affinity to an ADP affinity. The V159I mutant ATP-affinity didn't change because oxidant was needed to oxidant (NaN3/D-Deoxyglucose) to produce clusters. One of the failed essays, the analog-ATP, could be used in an In-vivo study to ensure our results.

4.2 Future work

While the HeLa cell study was a success, we would like to introduce additional mutants in the nucleotide binding pocket of actin to explore if there are additional residues that introduce ADP-actin-like behavior. Another possible experiment is to see how our optogenetic constructs behave over time intervals longer than the ones utilized in this work to monitor whether optogenetic cofilin-actin rods retain their reversibility long-term. What is also essential that we expand the studies to a neural cell and cultured neurons so the big question can be answered, what is the role of cofilin-actin rods in AD? To do this, we must have the biologically relevant cell line; possible choices are Neuro-2a or SH-SY5Y. Neuro-2a cells originate from a mouse and can exhibit responses to toxins which includes our oxidant. The cell line has been used to study neurite outgrowth and Alzheimer's disease More studies into how cofilin-actin rods affect other AD precursors such as Aβ peptides, tau peptide, and tau phosphorylation would be of interest. We should also explore how our constructs affect neuronal viability and function. Overall, we have shown that we have created a protocol and an optogenetic construct where we can recreate the phenomena of cofilin-actin rods. We have created optogenetics constructs that are reversible when exposed to blue light and a way to screen for compounds to prevent rod formation. Future works can finally answer the question of how rods play a role in Alzheimer's Disease.

References

1. Bamburg JR, Bernstein BW. Actin dynamics and cofilin-actin rods in alzheimer disease. Cytoskeleton. 2016;73(9):477-97.

2. Dickson DW. Introduction to Neurodegeneration: The Molecular Pathology of Dementia and Movement Disorders. In: Neurodegeneration: The Molecular Pathology of Dementia and Movement Disorders. Wiley-Blackwell; 2011. p. 1-5.

3. Crews L, Masliah E. Molecular mechanisms of neurodegeneration in Alzheimer's disease. Human molecular genetics. 2010 Apr 15, 19(R1):R20.

4. J. F. R KERR, A. H. WYLLIE, A. R. CURRIE From D P, U A. APOPTOSIS: A BASIC BIOLOGICAL PHENOMENON WITH WIDE- RANGING IMPLICATIONS IN TISSUE KINETICS. Br. J. Cancer. 1972;26.

5. Alberts B. Molecular biology of the cell. Sixth ed. New York, NY: Garland Science, Taylor and Francis Group; 2015.

6. Pivtoraiko VN, Roth KA. Cell Death and Neurodegeneration. In: Neurodegeneration: The Molecular Pathology of Dementia and Movement Disorders. Wiley-Blackwell; 2011. p. 6-9.

7. Elmore S. Apoptosis: A Review of Programmed Cell Death. Toxicologic Pathology. 2007 Jun;35(4):495-516.

8. Birben E, Sahiner UM, Sackesen C, Erzurum S, Kalayci O. Oxidative stress and antioxidant defense. The World Allergy Organization journal. 2012 Jan;5(1):9-19.

9. Knopman D. Clinical Aspects of Alzheimer's Disease. In: Neurodegeneration: The Molecular Pathology of Dementia and Movement Disorders. Wiley-Blackwell; 2011. p. 37-50.

10. McCord JM, Fridovich I. Superoxide dismutase. An enzymic function for erythrocuprein (hemocuprein). The Journal of biological chemistry. 1969 Nov 25,;244(22):6049.

11. Markesbery WR, Carney JM. Oxidative Alterations in Alzheimer's Disease. Brain Pathology. 1999 Jan;9(1):133-46.

12. McKhann G, Drachman D, Folstein M, Katzman R, Price D, Stadlan EM. Clinical diagnosis of Alzheimer's disease: report of the NINCDS-ADRDA Work Group under the auspices of Department of Health and Human Services Task Force on Alzheimer's Disease. Neurology. 1984 Jul;34(7):939.

13. Finder VH, Glockshuber R. Amyloid-[beta] Aggregation. Neuro - Degenerative Diseases. 2007;4(1):13-27.

14. Barnham KJ, Masters CL, Bush AI. Neurodegenerative diseases and oxidatives stress. Nature Reviews Drug Discovery. 2004;3(3):205-14.

15. Perry G, Mondragn-Rodrguez S, Nunomura A, Zhu X, Moreira PI, Smith MA. Oxidative Stress and Balance in Neurodegenerative Diseases. In: Neurodegeneration: The Molecular Pathology of Dementia and Movement Disorders. Wiley-Blackwell; 2011. p. 10-2.

16. Bamburg JR, Bernstein BW. Roles of ADF/cofilin in actin polymerization and beyond. F1000 biology reports. 2010;2:62.

17. Korn ED, Carlier MF, Pantaloni D. Actin polymerization and ATP hydrolysis. Science. 1987;238(4827):638-44.

18. Mannherz HG. The actin cytoskeleton and bacterial infection. Cham, Switzerland: Springer; 2017.

19. Actin: Structure, Functions, and Disease. Consuelas VA and Minas DJ, editors. Hauppauge: Nova Science Publishers, Inc.; 2012.

20. Kudryashov DS, Reisler E. ATP and ADP actin states. Biopolymers. 2013 Apr;99(4):245-56.

21. Dominguez R, Holmes KC. Actin Structure and Function. Annual review of biophysics. 2011;40:169-86.

22. Winder SJ, Ayscough KR. Actin-binding proteins. Journal of cell science. 2005 Feb 15,;118(Pt 4):651-4.

23. Bamburg JR, Wiggan OP. ADF/cofilin and actin dynamics in disease. Trends in Cell Biology. 2002;12(12):598-605.

24. Van Troys M, Huyck L, Leyman S, Dhaese S, Vandekerkhove J, Ampe C. Ins and outs of ADF/cofilin activity and regulation. European Journal of Cell Biology. 2008;87(8):649-67.

25. Pivovarova AV, Chebotareva NA, Kremneva EV, Lappalainen P, Levitsky DI. Effects of actin-binding proteins on the thermal stability of monomeric actin. Biochemistry. 2013 January;52(1):152-60.

26. H J Kinosian, L A Selden, J E Estes, L C Gershman. Nucleotide binding to actin. Cation dependence of nucleotide dissociation and exchange rates. Journal of Biological Chemistry. 1993 Apr 25,;268(12):8683.

27. Schüler H, Lindberg U, Schutt CE, Karlsson R. Thermal unfolding of G-actin monitored with the DNase I-inhibition assay stabilities of actin isoforms. European journal of biochemistry. 2000 January;267(2):476-86.

28. Hughes RM, Lawrence DS. Optogenetic Engineering: Light-Directed Cell Motility. Angewandte Chemie International Edition. 2014 Oct 6,;53(41):10904-7.

29. Kara Rodgers,. Gel Electrophoresis.

30. Masek T, Vopalensky V, Suchomelova P, Pospisek M. Denaturing RNA electrophoresis in TAE agarose gels. Analytical Biochemistry. 2005;336(1):46-50.

31. Hames BD. Gel Electrophoresis of Proteins: A Practical Approach. England: Oxford University Press; 1998.

32. Greenfield NJ. Using circular dichroism spectra to estimate protein secondary structure. Nat Protoc. 2006;1(6):2876-90.

33. Kelly SM, Jess TJ, Price NC. How to study proteins by circular dichroism. BBA - Proteins and Proteomics. 2005;1751(2):119-39.

34. Counterman AE, Clemmer DE, Thompson MS. Identifying a protein by MALDI-TOF mass spectrometry: an experiment for the undergraduate laboratory. Journal of Chemical Education. 2003 Feb 1,;80(2):177.

35. Calderaro A, Arcangeletti M, Rodighiero I, Buttrini M, Gorrini C, Motta F, et al. Matrix-assisted laser desorption/ionization time-of-flight (MALDI-TOF) mass spectrometry applied to virus identification. Scientific reports. 2014;4(1):6803.

36. Rosano GL, Ceccarelli EA. Recombinant protein expression in Escherichia coli: advances and challenges. Frontiers in Microbiology. 2014;5:172.

37. Stevens RC. Design of high-throughput methods of protein production for structural biology. Structure. 2000;8(9):R185.

38. Bornhorst JA, Falke JJ. 16] Purification of Proteins Using Polyhistidine Affinity Tags. Meth Enzymol. 2000;326:245-54.

39. Wingfield PT. Overview of the purification of recombinant proteins. Current protocols in protein science / editorial board, John E. Coligan ... [et al.]. 2015;80:6.1.1.

40. Palmer I, Wingfield PT. Preparation and extraction of insoluble (inclusion-body) proteins from Escherichia coli. Current protocols in protein science / editorial board, John E. Coligan ... [et al.]. 2004 Nov;Chapter 6:Unit 6.3.

41. Pastrana E. Optogenetics: controlling cell function with light. Nature Methods. 2011 Jan;8(1):24-5.

42. Optogenetics Guide [Internet]. []. Available from: https://www.addgene.org/optogenetics/guide/.

43. Illuminating cell biology: a how-to guide to optogenetics [Internet].; 2016 [cited 4/23/2018]. Available from: https://blog.benchling.com/2016/08/03/illuminating-cell-biology-a-how-to-guide-to-optogenetics/.

44. Wilson DF, Chance B. Azide inhibition of mitochondrial electron transport I. The aerobic steady state of succinate oxidation. Biochimica et Biophysica Acta (BBA) - Bioenergetics. 1967;131(3):421-30.

45. Voytek Okreglak, David G. Drubin. Cofilin Recruitment and Function during Actin-Mediated Endocytosis Dictated by Actin Nucleotide State. The Journal of Cell Biology. 2007 Sep 24,;178(7):1251-64.

46. Jianjie Mi, Alisa E Shaw, Chi W Pak, Keifer P Walsh, Laurie S Minamide, Barbara W Bernstein, et al. A Genetically Encoded Reporter for Real-Time Imaging of Cofilin-Actin Rods in Living Neurons. PLoS One. 2013 Dec 1,;8(12):e83609.

47. Nagy A. Cre recombinase: the universal reagent for genome tailoring. Genesis (New York, N.Y. : 2000). 2000 Feb;26(2):99-109.

48. Robert M Hughes, David J Freeman, Kelsey N Lamb, Rebecca M Pollet, Weston J Smith, David S Lawrence. Optogenetic Apoptosis: Light-Triggered Cell Death. Angewandte Chemie. 2015 Oct 5,;127(41):12232.

49. Lipofectamine® 3000 Reagent Protocol. 2014.

50. Khadijeh Falahzadeh, Amir Banaei-Esfahani, Maryam Shahhoseini. The Potential Roles of Actin in The Nucleus. Cell Journal. 2015 Apr 1,;17(1):7.